Renormalization of the NN interaction with a chiral two-pion exchange potential. II. Noncentral phases

M. Pavón Valderrama and E. Ruiz Arriola
Departamento de Física Atómica, Molecular y Nuclear, Universidad de Granada, E-18071 Granada, Spain
(Received 16 June 2006; published 26 December 2006)

We extend the renormalization of the NN interaction with chiral two-pion exchange potential to the calculation of noncentral partial wave phase shifts with total angular momentum $j \leqslant 5$. The short distance singularity structure of the potential, as well as the requirement of orthogonality conditions on the wave functions, determines exactly the number of undetermined parameters after renormalization.

DOI: 10.1103/PhysRevC.74.064004 PACS number(s): 21.30.Fe, 03.65.Nk, 11.10.Gh, 13.75.Cs

I. INTRODUCTION

The original proposal by Weinberg [1,2], which was carried out for the first time by Ray, Ordoñez, and van Kolck [3], of making model-independent predictions for NN scattering using chiral perturbation theory (ChPT) has been followed by a wealth of works [4–28] (for a review, see, e.g., Ref. [29]). The renormalized potential as given in Refs. [3–5] in configuration space is expanded taking $m^2/16\pi^2 f^2$ and m/M as small parameters (m and M are the pion and nucleon masses, respectively, and f is the pion weak decay constant), with mr fixed. In this counting for the potential and in a given partial wave (coupled) channel with good total angular momentum, the reduced potential can schematically be written as

$$U(r) = Mm\left\{\frac{m^2}{f^2}W^{(0)}(mr) + \frac{m^4}{f^4}W^{(2)}(mr) + \frac{m^4}{f^4}\frac{m}{M}W^{(3)}(mr) + \cdots\right\}, \quad (1)$$

where $W^{(n)}$ are known dimensionless functions which are everywhere finite except for the origin and depend on the axial coupling constant. $W^{(3)}$ depends also on three additional low-energy constants, $\bar{c}_1 = c_1 M$, $\bar{c}_3 = c_3 M$, and $\bar{c}_4 = c_4 M$, which have been determined from πN-scattering ChPT studies in a number of works [30–33].

At the level of approximation of Eq. (1), these potentials are local and energy independent and become singular at the origin. Thus, nonperturbative renormalization methods must be applied to give a precise meaning to the scattering amplitude [34] (for a comprehensive review in the one channel case, see, e.g., Ref. [35], and see Ref. [36] for a modern perspective). Several methods have been proposed to study the Leading Order (LO) term in Eq. (1) for central [37–41] and noncentral [42] waves. Recently [41,43], we showed how a renormalization program can be carried out for the NN interaction for the one-pion exchange (OPE) and chiral two-pion exchange (TPE) potentials in the central ${}^1S_0$ and ${}^3S_1$-${}^3D_1$ waves and its implications for the deuteron and pion-deuteron scattering [44]. In the present work, we extend our analysis to all remaining partial waves with $j \leqslant 5$ for both the OPE and chiral TPE potentials. As we showed in Refs. [41,43], the short distance behavior of the chiral NN potential, Eq. (1), determines exactly how many counterterms are needed to generate renormalized and finite, i.e., cutoff independent, phase shifts. These counterterms can be determined by fixing some low-energy parameters while the cutoff is removed. It has been assumed that dimensional power counting in the counterterms can be made independently of the short distance singularity of the potential. This yields conflicts between naive dimensional power counting and renormalization, which have been reported recently even for low partial waves [42]. So, one is led to two alternatives: either keep the power counting and a finite cutoff or remove the cutoff at the expense of modifying the power counting of the short distance interaction. The finite cutoff route has been explored in great detail in the past [5–10]. In this paper, we explore further the possibility of taking the alternative suggested by renormalization and the tight constraints imposed by finiteness. The analysis becomes rather transparent in coordinate space, where the counterterms can be mapped into boundary conditions [39,40,45] at the origin. In practice, renormalization may be carried out in several ways. In coordinate space, it seems natural to exploit the locality of the long distance (renormalized) potentials and then to renormalize the full scattering problem. In the present work, we adhere to this two-step renormalization, which has the additional advantage of making it possible to determine *a priori* and based on simple analytical arguments the existence of the renormalized limit and how many independent renormalization conditions (counterterms) are compatible with this limit. In this regard, let us recall that the main advantage of renormalization is that identical finite and unique results should be obtained regardless of the method of calculation (coordinate or momentum space) and regularization provided the same input physical data are used to eliminate the divergencies. In particular, we also expect independence of the way in which the limit is taken.

The origin of the conflict can be traced back to the question of whether for a given energy-independent local potential, such as Eq. (1), one can assume any short distance physics regardless of the form of the long range potential. Renormalization group invariance, however, requires that any physical parameter sit on a renormalization trajectory and that the corresponding evolution on the renormalization scale be dictated by the form of the long distance potential at

*Electronic address: mpavon@ugr.es
†Electronic address: earriola@ugr.es

all distances. The precise trajectory is uniquely fixed by a renormalization condition at very long distances. Thus, the separation between the short and long distance contributions is not only scale dependent but also potential dependent [39,40]. Renormalization conditions are physical and do not exhibit this dependence. Finiteness of the scattering amplitude and orthogonality of scattering (and eventually bound state) wave functions impose very tight constraints on the allowed number of counterterms and their possible scale dependence [41,43]. The discussion becomes rather straightforward in coordinate space and in terms of boundary conditions for ordinary differential equations. In addition, unlike momentum space treatments, a very natural hierarchy of the renormalization problem takes place in configuration space [41,43]. More specifically, orthogonality of different energy solutions requires an energy-independent boundary condition on the wave function for the long distance local and energy-independent potentials, as is the case for Eq. (1) valid to Next to Next to Leading Order (NNLO), so that in all cases, the effective range and higher order threshold parameters cannot be taken as independent input parameters.[1]

The results found in Refs. [41,43] can be concisely summarized as follows in the one channel case. For a regular potential, i.e., one diverging less strongly than the inverse square potential, $r^2|U(r)| < \infty$, one may choose between the regular and irregular solutions. In the first case, the scattering length is predicted; while in the second case, the scattering length becomes an input of the calculation. Singular potentials at the origin, i.e., fulfilling $r^2|U(r)| \to \infty$, do not allow this choice. If the potential is repulsive, the scattering length depends on the potential; while for an attractive potential, the scattering length must be chosen as an independent parameter. In the coupled channel situation, one must look at the strongest singularity of the potential eigenvalues at the origin and apply the single channel results.

In our formulation of the NN renormalization problem, threshold parameters play an essential role. Unfortunately, scattering threshold parameters for higher partial waves other than the S waves have never been considered in the context of chiral potentials [5–10]. Instead, some calculations adjust their counterterms to fit the phase shifts in the region above threshold to the Nijmegen database [46,47]. In a recent work, we filled the gap by carrying out a complete determination of these threshold parameters for the Reid93 and NijmII potentials [48]. In light of this new information, it is quite possible that the good fits in the intermediate-energy region imply a somewhat less accurate description in the threshold region. This issue will become relevant in the description of some partial waves.

The paper is organized as follows. In Sec. II, we review the formalism for coupled channel scattering in the presence of singular potentials at the origin. For completeness, we list the potentials in Appendix A. Based on the short distance behavior of those potentials (see Appendix B) and the requirement of orthogonality, we determine the number of independent parameters for any partial wave with $j \leqslant 5$. In Sec. III, we present our results for the phase shifts. Specifically, we make a thorough analysis of cutoff dependence in all partial waves, for both for the OPE and the chiral TPE potentials. We also discuss the perturbative nature of peripheral waves within the present nonperturbative approach. Finally, in Sec. IV we present our conclusions.

II. FORMALISM

We solve the coupled channel Schrödinger equation for relative motion, which in compact notation reads

$$-\mathbf{u}''(r) + \left[\mathbf{U}(r) + \frac{\mathbf{l}^2}{r^2}\right]\mathbf{u}(r) = k^2\mathbf{u}(r), \tag{2}$$

where $\mathbf{U}(r) = 2\mu_{np}\mathbf{V}(r)$ is the coupled channel matrix reduced potential, with $\mu_{np} = M_p M_n/(M_p + M_n)$, which is the reduced proton-neutron mass. For $j > 0$, it can be written as

$$\mathbf{U}^{0j}(r) = U^{0j}_{jj},$$
$$\mathbf{U}^{1j}(r) = \begin{pmatrix} U^{1j}_{j-1,j-1}(r) & 0 & U^{1j}_{j-1,j+1}(r) \\ 0 & U^{1j}_{jj}(r) & 0 \\ U^{1j}_{j-1,j+1}(r) & 0 & U^{1j}_{j+1,j+1}(r) \end{pmatrix}. \tag{3}$$

In Eq. (2), $\mathbf{l}^2 = \mathrm{diag}[l_1(l_1+1), \ldots, l_N(l_N+1)]$ is the orbital angular momentum, $\mathbf{u}(r)$ the reduced matrix wave function, k the c.m. momentum, and j the total angular momentum. In our case, $N = 1$ for the spin singlet channel with $l = j$, and $N = 3$ for the spin triplet channel with $l_1 = j-1$, $l_2 = j$, and $l_3 = j+1$. The potentials used in this paper were obtained in Refs. [3–5] in coordinate space and are listed in Appendix A for completeness.

A. Long distance behavior

At long distances, we assume the usual asymptotic normalization condition

$$\mathbf{u}(r) \to \hat{\mathbf{h}}^{(-)}(r) - \hat{\mathbf{h}}^{(+)}(r)\mathbf{S}, \tag{4}$$

with $\mathbf{S}$ the coupled channel unitary S matrix. The corresponding outgoing and ingoing free spherical waves are given by

$$\hat{\mathbf{h}}^{(\pm)}(r) = \mathrm{diag}(\hat{h}^{\pm}_{l_1}(kr), \ldots, \hat{h}^{\pm}_{l_N}(kr)), \tag{5}$$

with $\hat{h}^{\pm}_l(x)$ the reduced Hankel functions of order l, $\hat{h}^{\pm}_l(x) = x H^{\pm}_{l+1/2}(x)[\hat{h}^{\pm}_0(x) = e^{\pm ix}]$, and they satisfy the free Schrödinger's equation for a free particle.

For the spin singlet state $s = 0$, one has $l = j$, and hence the state is uncoupled, that is,

$$S^{0j}_{jj} = \exp\left(2i\delta^{0j}_j\right), \tag{6}$$

whereas for the spin triplet state $s = 1$, one has the uncoupled $l = j$ state, that is,

$$S^{1j}_{jj} = \exp\left(2i\delta^{1j}_j\right), \tag{7}$$

and the two channel coupled $l, l' = j \pm 1$ states for which we use Stapp-Ypsilantis-Metropolis (SYM or nuclear bar) [49] parametrization

[1] Actually, the potential in Eq. (1) contains distributional contributions, which strictly speaking are zero for any finite distance. See the discussion in our previous work [43].

$$S^{1j} = \begin{pmatrix} S^{1j}_{j-1j-1} & S^{1j}_{j-1j+1} \\ S^{1j}_{j+1j-1} & S^{1j}_{j+1j+1} \end{pmatrix} = \begin{pmatrix} \cos(2\bar{\epsilon}_j)\exp\left(2i\bar{\delta}^{1j}_{j-1}\right) & i\sin(2\bar{\epsilon}_j)\exp\left[i\left(\bar{\delta}^{1j}_{j-1}+\bar{\delta}^{1j}_{j+1}\right)\right] \\ i\sin(2\bar{\epsilon}_j)\exp\left[i\left(\bar{\delta}^{1j}_{j-1}+\bar{\delta}^{1j}_{j+1}\right)\right] & \cos(2\bar{\epsilon}_j)\exp\left(2i\bar{\delta}^{1j}_{j+1}\right) \end{pmatrix}$$

In the discussion of low-energy properties, we also use the Blatt-Biedenharn (BB or eigenphase) parametrization [50] defined by

$$S^{1j} = \begin{pmatrix} \cos\epsilon_j & -\sin\epsilon_j \\ \sin\epsilon_j & \cos\epsilon_j \end{pmatrix} \begin{pmatrix} \exp\left(2i\delta^{1j}_{j-1}\right) & 0 \\ 0 & \exp\left(2i\delta^{1j}_{j+1}\right) \end{pmatrix} \times \begin{pmatrix} \cos\epsilon_j & \sin\epsilon_j \\ -\sin\epsilon_j & \cos\epsilon_j. \end{pmatrix}. \tag{8}$$

The relation between the BB and SYM phase shifts is

$$\bar{\delta}^{1j}_{j+1} + \bar{\delta}^{1j}_{j-1} = \delta^{1j}_{j+1} + \delta^{1j}_{j-1}, \tag{9}$$

$$\sin\left(\bar{\delta}^{1j}_{j-1} - \bar{\delta}^{1j}_{j+1}\right) = \frac{\tan(2\bar{\epsilon}_j)}{\tan(2\epsilon_j)}. \tag{10}$$

In the present paper, zero-energy scattering parameters play an essential role since they are often used (see below) as input parameters of the calculation of phase shifts. Due to unitarity of the S matrix in the low-energy limit, $k \to 0$, we have

$$(\mathbf{S}-\mathbf{1})_{l',l} = -2i\alpha_{l',l}k^{l'+l+1} + \cdots, \tag{11}$$

with $\alpha_{l'l}$ the (Hermitian) scattering length matrix.[2] The threshold behavior acquires its simplest form in the SYM representation

$$\delta^{0j}_j \to -\alpha^{0j}_j k^{2j+1}, \tag{12}$$

$$\delta^{1j}_j \to -\alpha^{1j}_j k^{2j+1}, \tag{13}$$

$$\bar{\delta}^{1j}_{j-1} \to -\bar{\alpha}^{1j}_{j-1} k^{2j-1}, \tag{14}$$

$$\bar{\delta}^{1j}_{j+1} \to -\bar{\alpha}^{1j}_{j+1} k^{2j+3}, \tag{15}$$

$$\bar{\epsilon}_j \to -\bar{\alpha}^{1j}_j k^{2j+1}. \tag{16}$$

In the BB form, one has similar behaviors for the δ's, but ϵ_j behaves as k^{2j} instead of k^{2j+1}, that is,

$$\delta^{1j}_{j-1} \to -\bar{\alpha}^{1j}_{j-1} k^{2j-1}, \tag{17}$$

$$\delta^{1j}_{j+1} \to -\left(\bar{\alpha}^{1j}_{j+1} - \frac{\left(\bar{\alpha}^{1j}_j\right)^2}{\bar{\alpha}^{1j}_{j-1}}\right) k^{2j+3}, \tag{18}$$

$$\epsilon_j \to \frac{\bar{\alpha}^{1j}_j}{\bar{\alpha}^{1j}_{j-1}} k^{2j}. \tag{19}$$

[2]For non-S-wave scattering, the dimension of $\alpha_{l,l'}$ is $\mathrm{fm}^{l+l'+1}$ which is not a length. For simplicity, though, we will call them scattering lengths.

B. Short distance behavior

The form of the wave function at the origin is uniquely determined by the form of the potential at short distances (see, e.g., Refs. [34,35] for the case of one channel and Refs. [41,43] for coupled channels). For the chiral NN potential, Eq. (1), one has

$$\mathbf{U}_{\mathrm{LO}}(r) \to \frac{M\mathbf{C}_{3,\mathrm{LO}}}{r^3},$$

$$\mathbf{U}_{\mathrm{NLO}}(r) \to \frac{M\mathbf{C}_{5,\mathrm{NLO}}}{r^5},$$

$$\mathbf{U}_{\mathrm{NNLO}}(r) \to \frac{M\mathbf{C}_{6,\mathrm{NNLO}}}{r^6}, \tag{20}$$

where LO includes the first term in Eq. (1), NLO the first two terms, and so on. Note that higher order potentials become increasingly singular at the origin. For a potential diverging at the origin as an inverse power law, one has

$$\mathbf{U}(r) \to \frac{M\mathbf{C}_n}{r^n}, \tag{21}$$

with $\mathbf{C}_n$ a matrix of generalized van der Waals coefficients and $n > 2$ an integer. One diagonalizes the matrix $\mathbf{C}_n$ by a constant unitary transformation $\mathbf{G}$, yielding

$$M\mathbf{C}_n = \mathbf{G}\,\mathrm{diag}\left(\pm R_1^{n-2}, \ldots, \pm R_N^{n-2}\right)\mathbf{G}^{-1}, \tag{22}$$

with R_i constants with length dimension. The plus sign corresponds to the case with a positive eigenvalue (repulsive) and the minus sign to the case with a negative eigenvalue (attractive). Then, at short distances, one has the solutions

$$\mathbf{u}(r) \to \mathbf{G}\begin{pmatrix} u_{1,\pm}(r) \\ \cdots \\ u_{N,\pm}(r) \end{pmatrix}, \tag{23}$$

where for the attractive and repulsive cases, one has

$$u_{i,-}(r) \to C_{i,-}\left(\frac{r}{R_i}\right)^{n/4} \sin\left[\frac{2}{n-2}\left(\frac{R_i}{r}\right)^{\frac{n}{2}-1} + \varphi_i\right], \tag{24}$$

$$u_{i,+}(r) \to C_{i,+}\left(\frac{r}{R_i}\right)^{n/4} \exp\left[-\frac{2}{n-2}\left(\frac{R_i}{r}\right)^{\frac{n}{2}-1}\right], \tag{25}$$

respectively. This behavior of the wave functions near the origin is valid regardless of the energy, provided the distances are small enough.[3] Here, φ_i are arbitrary short distance phases which in general depend on the energy. There are as many

[3]In fact, the next correction to the near-the-origin wave functions, which is energy dependent, is suppressed by a relative $(kR)^2(r/R)^{n/2+1}$ power with respect to the main term, so it is negligible in the $r \to 0$ limit.

short distance phases as there are short distance attractive eigenpotentials. Orthogonality of the wave functions at the origin yields the relation

$$\sum_{i=1}^{N}[u_{k,i}{}^{*}u'_{p,i} - u'_{k,i}{}^{*}u_{p,i}]|_{r=0} = \sum_{i=1}^{A}\cos(\varphi_i(k) - \varphi_i(p)), \tag{26}$$

where $A \leqslant N$ is the number of short distance attractive eigenpotentials.

The simplest choice for fixing relative phases for a positive-energy scattering state is to take the zero-energy state $p = 0$ as a reference state and the zero-energy short distance phase. In the particular case in which only one eigenvalue is negative, the short distance phase is energy independent. This may happen both in the singlet as well as in the triplet channels with $j = l$. The short distance phase is then fixed by reproducing the scattering length in the singlet channel and one of the three scattering lengths in the triplet channel. In the case having two negative, i.e., attractive, eigenvalues (this can only happen in triplet channels), there are two undetermined short distance phases which can be fixed by using the corresponding three scattering lengths. The case of two positive, i.e., repulsive, eigenvalues does not allow one to fix any scattering length. The case with two different signs for the eigenvalues fixes only one scattering length. Note that in this construction and for two coupled channels, there is no intermediate situation in which the solution is specified by just two scattering lengths; one has only zero, one, or three.

Although our arguments are entirely based on analytical calculations, our conclusions agree with the findings in Ref. [42] for the OPE case. There, counterterms beyond those dictated by Weinberg's power counting are included in the ${}^3P_0$, ${}^3P_2$-${}^3F_2$, and ${}^3D_2$ waves to ensure renormalizability on numerical grounds. As we will see below, our renormalized phase shifts for the special OPE case reproduce essentially their results, although our TPE nonperturbatively renormalized amplitudes go beyond these results.

Another issue is that of the establishment of a theoretically compelling and mathematically consistent power counting which also provides phenomenological success. This has been the goal of much of the EFT activity in recent years. Despite the fact that our OPE is mathematically identical to the one in Ref. [42], where a strong emphasis on power counting has been made, our motivation is slightly different. Actually, these authors argue that a consistent scheme for TPE might be achieved within a perturbative framework, using the nonperturbative OPE distorted amplitudes as the leading order approximation. This is theoretically appealing, and the issue was thoroughly discussed within the coordinate space approach in our previous paper on the central waves [43]. There, we pointed out that with enough counterterms, such a program could be pursued, although orthogonality was violated and results did not exhibit a clear improvement over the fully iterated potentials. The reason was the appearance of nonanalytical dependences on the would-be dimensional power counting parameter, a situation that had not been foreseen in the standard EFT setup. This suggests that the discussion on power counting and the systematics of EFT is not yet over. Therefore, as we did in our previous work, we focus more on establishing long range model-independent correlations, leaving the possible establishment of a satisfactory power counting for future studies.

C. Regularization methods

In principle, one can implement the short distance behavior of the wave functions, Eq. (25), if one goes to sufficiently small distances or if the short distance behavior of the the wave function is improved [41]. Computationally, the implementation of short distance regulators is mostly straightforward. The attractive or repulsive nature of the potentials at short distances requires different choices of regulators [41,43]. For a one-channel repulsive singular potential, we use the regulator

$$\frac{u'_k(a)}{u_k(a)} = \frac{l+1}{a}. \tag{27}$$

This condition ensures orthogonality of wave functions with different energy. For the attractive singular case, we integrate in from infinity at zero energy down to a given boundary radius a, impose orthogonality at the boundary by matching logarithmic derivatives

$$\frac{u'_k(a)}{u_k(a)} = \frac{u'_0(a)}{u_0(a)}, \tag{28}$$

and then integrate out at finite energy. In the coupled channel case, we extend the method by applying the one channel regularization to the short distance eigenfunctions, Eq. (23).

D. Fixing of parameters and renormalization conditions

Fixing the short distance phases requires some renormalization conditions. As we have said, an appealing choice is to impose this condition at zero energy. The way to proceed in practice is quite straightforward though tedious given the large number (27) of partial waves considered in this work. In the singlet channel case and for an attractive short distance singularity, one starts at zero energy and integrates in from large distances of $\sim$15 fm with a given scattering length until a short boundary radius of $\sim$0.1 fm. At finite energy, one integrates out, matching the wave function to the zero-energy solution at the short distance boundary generating a phase shift from a given prescribed scattering length. Of course, in this method, one has to check for cutoff independence (taking $r = 0.1$–0.2 fm proves to be enough). For the coupled channel case, one proceeds along similar lines; the procedure has been described in great detail in our previous works [41,43] for the $j = 1$ channel. The method relies heavily on the superposition principle of boundary conditions, and we use here the extension of that method to higher partial waves. One advantage of our approach is that we rarely have to make a fit to the data; any phase shift has by construction the right threshold behavior when the potential at short distances is attractive. For the repulsive potential case, the scattering length is predicted entirely from the potential. In any case, discrepancies with the data can be attributed to the potential.

TABLE I. Sets of chiral coefficients considered in this work.

Set	Source	$c_1(\mathrm{GeV}^{-1})$	$c_3(\mathrm{GeV}^{-1})$	$c_4(\mathrm{GeV}^{-1})$
I	πN [31]	−0.81	−4.69	3.40
II	NN [5]	−0.76	−5.08	4.70
III	NN [7]	−0.81	−3.40	3.40
IV	NN [8]	−0.81	−3.20	5.40

Inspection of Table I illustrates the situation for the LO, NLO, and NNLO approximations to the potential. We show the scattering lengths in all partial waves as determined in our previous work [48] together with the corresponding eigenvalues for the leading short distance coefficients in the LO (OPE), NLO, and NNLO approximations to the potential. In the NNLO, one must also specify the values of the chiral constants c_1, c_3, and c_4. We use for definiteness the values of Ref. [8], since, as we saw in Ref. [43], they provide a reasonable description of deuteron properties.

E. Details on the numerical procedure

The integration of the coupled differential equations requires some care, particularly in the vicinity of the short distance singularities. In the case of attractive singularities, because of the increasing oscillations, the wave function has to be sampled with great detail at a rate similar to the size of the oscillations. For the repulsive case, one must stop at sufficiently large distances because of the exponential suppression of the wave function. Another important condition has to do with preservation of in and out reversibility of the integration. This last requirement guarantees that for attractive channels, where the scattering length is supplied as an input parameter, the threshold behavior of the phase shift is consistent with that given scattering length.

Another problem one has to face for high partial waves is related to the practical influence of the scattering length on the calculated phase shifts. In principle, and for an attractive singular potential, the scattering length needs to be specified. For the one channel case, this is done by integrating in the zero-energy large distance solution, valid for $r \gg 2/m_\pi$,

$$u(r) \to r^{-l} - \frac{r^{l+1}}{\alpha_l}. \tag{29}$$

The long distance irregular solution dominates, unless α_l is anomalously large, i.e., $\alpha_l(m_\pi/2)^{(2l+1)} \gg 1$, so that when integrating in, much of the regular solution will be lost and the result will be rather insensitive to the value of α_l provided it is of normal size. This fact becomes relevant in the numerical calculations if the long distance cutoff is taken to be exceedingly large. To avoid this situation we take typically $R_{\max} = 15$ fm for large l.

III. RESULTS FOR PHASE SHIFTS

A. Numerical parameters

For our numerical calculations, we take $f_\pi = 92.4$ MeV, $m = 138.03$ MeV, $2\mu_{np} = M = M_p M_n/(M_p + M_n) = 938.918$ MeV, and $g_A = 1.29$ in the OPE piece to account for the Goldberger-Treimann discrepancy, and $g_A = 1.26$ in the TPE piece of the potential. The corresponding pion nucleon coupling constant takes, then, the value $g_{\pi NN} = 13.083$ (i.e., $g_A = 1.29$) according to the Nijmegen phase-shift analysis of NN scattering [51]. The values of the coefficients c_1, c_3, and c_4 used in this paper can be looked up in Table II for completeness. The potentials in configuration space used in this paper are exactly those provided in Refs. [3–5] but disregarding relativistic corrections, $M/E \to 1$.[4] The potentials are listed in Appendix A for completeness. The short distance van der Waals coefficients for all channels studied in the present work are presented in Appendix B. The output of such a channel-by-channel analysis is briefly summarized in Table II, where we indicate which scattering lengths are used as input parameters according to the discussion given in Sec. II. Low-energy parameters for the high quality potentials [46,47] have been obtained in Ref. [48]. We will use the NijmII values, but to give an idea of the expected lower uncertainties on those parameters, we

[4] As mentioned in our previous work [43] these effects are tiny for the deuteron. For central waves they are about 0.2° at the maximum c.m. momentum $p = 400$ MeV. This trend is general also for peripheral waves.

TABLE II. Number of independent parameters for different orders of approximation of the potential. Scattering lengths are in $\mathrm{fm}^{l+l'+1}$ and are taken from NijmII and Reid93 potentials [47] in Ref. [48]. We use the (SYM-nuclear bar) convention, Eq. (16).

Wave	α NijmII (Reid93)	LO	NLO	NNLO
$^1S_0$	−23.727(−23.735)	Input	Input	Input
$^3P_0$	−2.468(−2.469)	Input	–	Input
$^1P_1$	2.797(2.736)	–	–	–
$^3P_1$	1.529(1.530)	–	Input	Input
$^3S_1$	5.418(5.422)	Input	–	Input
$^3D_1$	6.505(6.453)	–	–	Input
E_1	1.647(1.645)	–	–	Input
$^1D_2$	−1.389(−1.377)	–	Input	Input
$^3D_2$	−7.405(−7.411)	Input	Input	Input
$^3P_2$	−0.2844(−0.2892)	Input	Input	–
$^3F_2$	−0.9763(−0.9698)	–	–	–
E_2	1.609(1.600)	–	–	–
$^1F_3$	8.383(8.365)	–	–	–
$^3F_3$	2.703(2.686)	–	Input	Input
$^3D_3$	−0.1449(−0.1770)	Input	–	Input
$^3G_3$	4.880(4.874)	–	–	Input
E_3	−9.695(−9.683)	–	–	Input
$^1G_4$	−3.229(−3.210)	–	Input	Input
$^3G_4$	−19.17(−19.14)	Input	Input	Input
$^3F_4$	−0.01045(−0.01053)	Input	Input	–
$^3H_4$	−1.250(−1.240)	–	–	–
E_4	3.609(3.586)	–	–	–
$^1H_5$	28.61(28.57)	–	–	–
$^3H_5$	6.128(6.082)	–	Input	Input
$^3G_5$	−0.0090(−0.010)	Input	–	Input
$^3I_5$	10.68(10.66)	–	–	Input
E_5	−31.34(−31.29)	–	–	Input

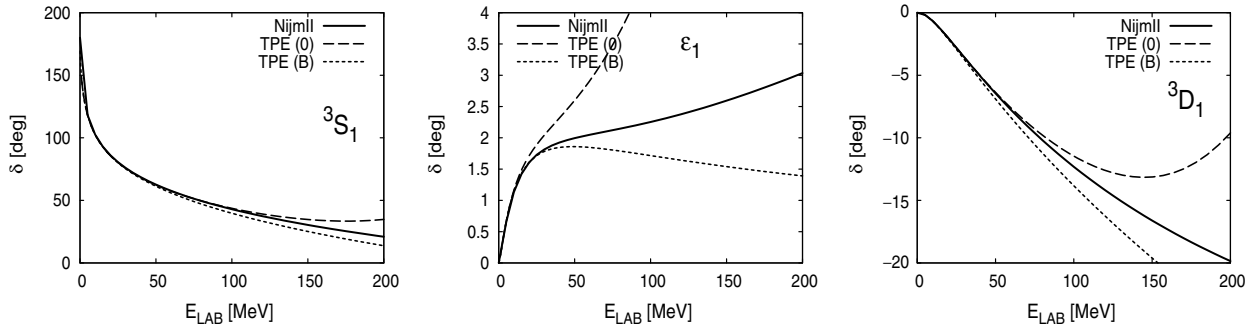

FIG. 1. Dependence of the $^3S_1$-$^3D_1$ channel (SYM-nuclear bar) phase shifts for the NNLO TPE potential on the reference state used to orthogonalize the scattering state compared with the corresponding phases of the database of Refs. [46,47]. Label TPE(0) means the zero-energy reference state with $\alpha_0 = 5.418$ fm, $\alpha_{02} = 1.647\,\mathrm{fm}^3$, and $\alpha_2 = 6.505\,\mathrm{fm}^5$. Label TPE(B) stands for the deuteron bound reference state with the experimental binding energy, asymptotic D/S ratio, together with $\alpha_0 = 5.418$ fm (corresponding to $\alpha_{02} = 1.67\,\mathrm{fm}^3$ and $\alpha_2 = 6.6\,\mathrm{fm}^5$ [43].)

also list the Reid93 values. Probably the real uncertainties are much larger since the actual value of these low-energy parameters will depend upon which long range physics is included in the high quality potentials where explicit TPE effects have not been included, as we do in the present work.[5]

B. The deuteron channel revisited

Before starting a full discussion of all partial waves, it is interesting to first reanalyze the $^3S_1$-$^3D_1$ channel already studied in our previous work on the deuteron [41,43]. There, we used the orthogonality to the deuteron bound state. The scattering lengths $\alpha_{02} = 1.67\,\mathrm{fm}^3$ and $\alpha_2 = 6.6\,\mathrm{fm}^5$ were deduced from the experimental deuteron binding energy, the asymptotic D/S ratio, and the S-wave scattering length α_0. These values turned out to be a bit off the values deduced from the NijmII and Reid93 potentials [45] (see Table II). Nevertheless, the intermediate-energy region turned out to be better described than the low-energy behavior suggested. In the present work, we choose instead to build scattering states which are orthogonal to the zero-energy states, so deuteron properties can be deduced, as done in Table III. In Fig. 1, we show the results when either the zero-energy or the deuteron bound state is used as the reference state. One obvious lesson from this comparison is that phase shifts, particularly the E_1 channel, may be better described in the intermediate-energy region if the deuteron is used as a reference state, despite the fact that the threshold behavior is a bit off. This is maybe explained by the observation that α_{02} and α_2 encode higher energy information about the system than α_0 or γ,[6] so the latter parameters are more suited to obtaining an effective description of the system. This feature will become evident in other partial waves.

C. Cutoff dependence

In Figs. 2–7, we show the results of our calculation for all partial waves with $j \leqslant 5$ as a function of the nucleon laboratory

[5]This will generate slight inconsistencies in the TPE results of Sec. III D3 which will be amended by a small modification of the threshold parameters, yet larger than the discrepancies between the threshold parameters for NijmII and Reid93 potentials obtained in Ref. [48].

[6]It should be note that α_{02} and α_2 are related to the behavior of the scattering amplitude at order k^2 and k^4, respectively, relative to α_0.

TABLE III. Deuteron properties for the OPE and TPE potentials. OPE(0) refers to the deuteron computed by orthogonality to the zero-energy scattering states, fixing α_0 to its experimental value; in OPE(B), the computation is made by fixing γ to its experimental value, constructing the corresponding bound state. Similarly, TPE(0) refers to the deuteron computed by orthogonality to zero-energy states, fixing α_0 to its experimental value and α_{02} and α_2 to their Nijmegen II values; in TPE(B), the computation is made by fixing γ, η, and α_0 to their experimental values. The errors quoted in OPE(0) correspond to the uncertainty in the value of the scattering length; in OPE(B), the errors correspond to changing the cutoff in the 0.1–0.2 fm range. Errors quoted in both TPE computations reflect the uncertainty in only the nonpotential parameters γ, η, and α_0. We take set IV [8] for the LEC's in the TPE calculation. Experimental values can be traced from Ref. [52].

Set	γ (fm^{-1})	η	A_S (fm$^{-1/2}$)	r_m (fm)	Q_d(fm^2)	P_D(%)	α_0 (fm)	α_{02}(fm^3)	α_2(fm^5)
OPE(0)	0.2274(4)	0.02564(4)	0.8568(10)	1.964(3)	0.2796(3)	7.208(12)	Input	1.754(7)	6.770(7)
OPE(B)	Input	0.02633	0.8681(1)	1.9351(5)	0.2762(1)	7.31(1)	5.335(1)	1.673(1)	6.693(1)
TPE(0)	0.2322(3)	0.02531(9)	0.8891(4)	1.968(3)	0.2723(3)	7.24(13)	Input	NijmII	NijmII
TPE(B)	Input	Input	0.884(4)	1.967(6)	0.276(3)	8(1)	Input	1.67(4)	6.6(4)
NijmII	0.231605	0.02521	0.8845	1.9675	0.2707	5.635	5.418	1.647	6.505
Reid93	0.231605	0.02514	0.8845	1.9686	0.2703	5.699	5.422	1.645	6.453
Exp.	0.231605	0.0256(4)	0.8846(9)	1.971(6)	0.2859(3)	–	5.419(7)	–	–

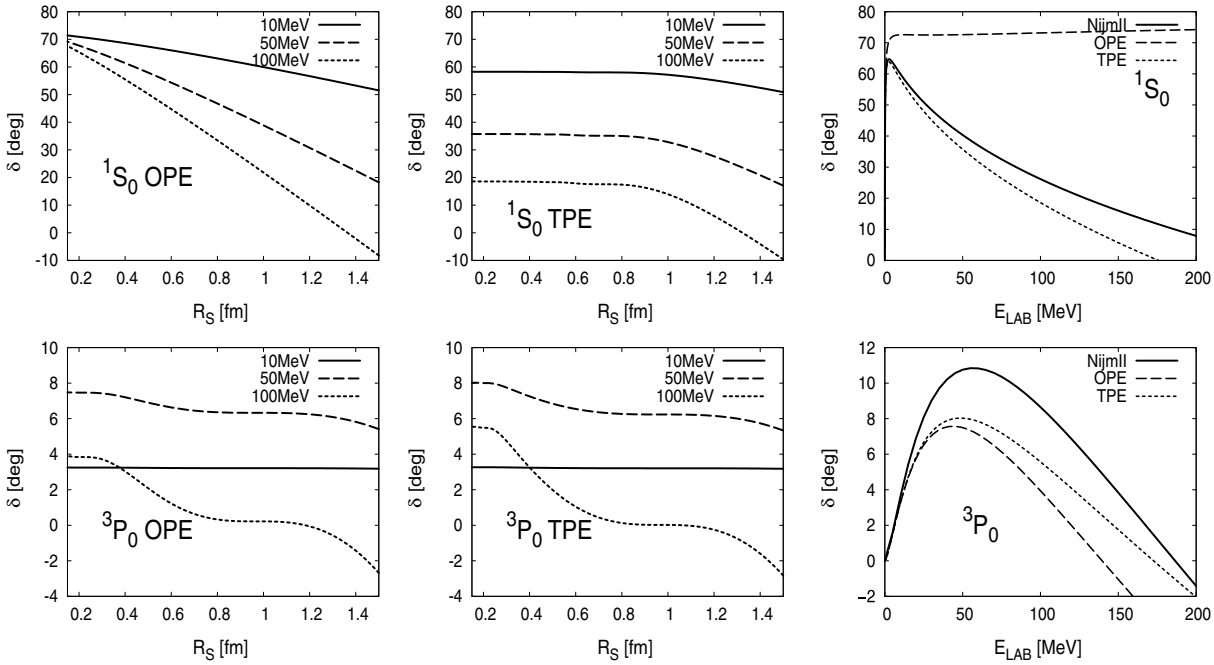

FIG. 2. *np* (SYM-nuclear bar) phase shifts for the total angular momentum $j = 0$. OPE (left) and chiral TPE (middle) as a function of the cutoff radius R_S for fixed laboratory energies, $E_{\rm LAB} = 10, 50, 100$ MeV. OPE and chiral TPE (right) renormalized (i.e., $R_S \to 0$) phase shifts as a function of $E_{\rm LAB}$ compared with the Nijmegen partial wave analysis [46,47].

energy. For definiteness, we use the chiral constants c_1, c_3, and c_4 of Ref. [8] (set IV), which already provided a good description of deuteron properties after renormalization [43] at NNLO. This choice allows a more straightforward comparison with the N^{3}LO calculation of Ref. [8] with finite cutoffs. Unless otherwise stated, the needed low-energy parameters for these figures are always taken to be those of Ref. [48] for the NijmII potential (see Table II).

To test the stability of the phase shifts against changes in the short distance cutoff parameter R_S, we show in Figs. 2–7 (similar to the OPE study in momentum space of Ref. [42]) the cutoff dependence for fixed values of the laboratory energy for both the OPE and TPE potentials. This is done in the range $0.15 \leqslant R_S \leqslant 1.5$ fm. If we identify this short distance cutoff with the sharp momentum cutoff $\Lambda = \pi/2R_S$ [45], the smallest boundary radius, $\sim$0.15 fm, corresponds to a maximum cutoff $\Lambda \sim 2$ GeV. This is much larger than the cutoffs used in Refs. [5–10] but comparable to the exponential cutoff used in Ref. [42] for the renormalization of the OPE potential.[7] Note that the limit $R_S \to 0$ may be taken independently for any different channel.

The evolution of the increasingly oscillating wave function in the attractive case can be identified with the cycles (improperly called limit cycles, see footnote 5 in Ref. [40]) described in Refs. [36,38,40,45] by looking at suitable logarithmic combinations of the wave functions. The cycles documented in Ref. [42] in momentum space can be mapped into the coordinate space cycles by relating the coordinate and momentum space cutoffs.

Generally speaking, the inclusion of chiral TPE effects generates smoother limits than those in the OPE results, as one would expect. We checked that for short distance repulsive (eigen)channels, results are not very sensitive to the choice of the regulator for small values of R_S. As we also see from the figures, the convergence depends both on the partial wave as well as on the energy. As expected, the needed value of the short distance cutoff R_S for which stability is achieved is rather high for peripheral waves, $R_S \sim 1/m_\pi$. Another feature of the calculation is the stability plateau observed for a number of partial waves. This trend has also been noted in previous works with finite cutoffs [11] where sequential cutoff windows appear. In coordinate space, this is originated by the almost self-similar pattern of the short distance oscillations of the wave function, which suggests a sequential and faster convergence modulo cycles [40].

Let us remark at this point that the existence of an $R_S \to 0$ limit does not necessarily mean a plateaulike approach to it. This is the case, for example, of the $^1S_0$ wave, which for OPE shows a linear dependence on the cutoff because of the mild $1/r$ singularity of the potential, generating a linearlike behavior which corresponds to the ratio of regular

[7]There, a cutoff has been introduced according to the rule in the potential $V(k', k) \to \exp(-k'^4/\Lambda^4)V(k'k)\exp(-k^4/\Lambda^4)$, and counterterms have been added. To get an order of magnitude of the equivalent sharp cutoff $\tilde{\Lambda}$, we estimate the linear divergence at zero energy in the contact theory,

$$\tilde{\Lambda} = \int_0^\infty \exp(-2q^4/\Lambda^2)dq = \frac{\Gamma(\frac{5}{4})}{2^{\frac{1}{4}}}\Lambda = 0.762\Lambda,$$

and using $\tilde{\Lambda} = \pi/2R_S$ [45], we get $\Lambda = 1/(0.48R_S)$.

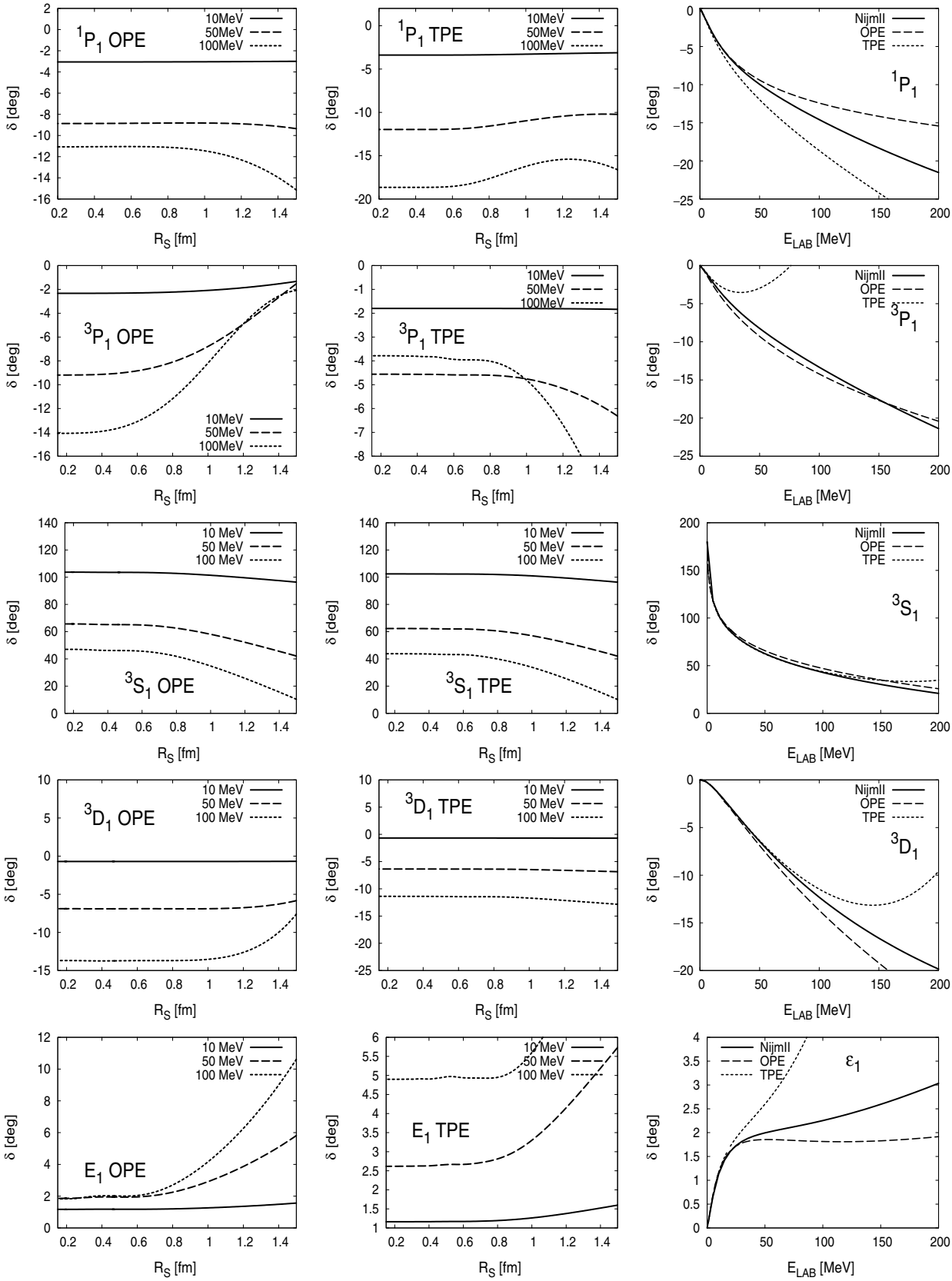

FIG. 3. Same as Fig. 2, but for $j = 1$.

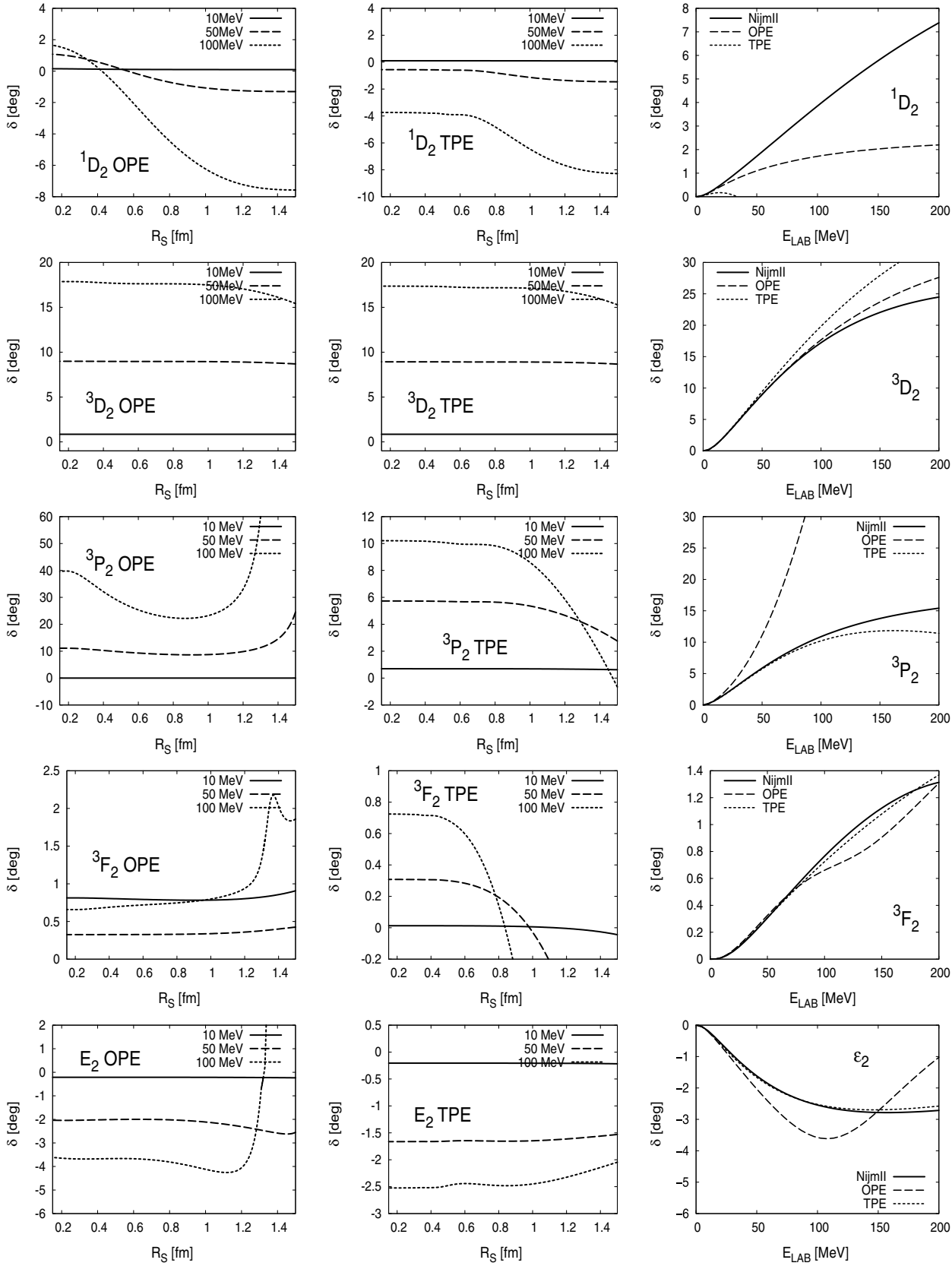

FIG. 4. Same as Fig. 2, but for $j = 2$.

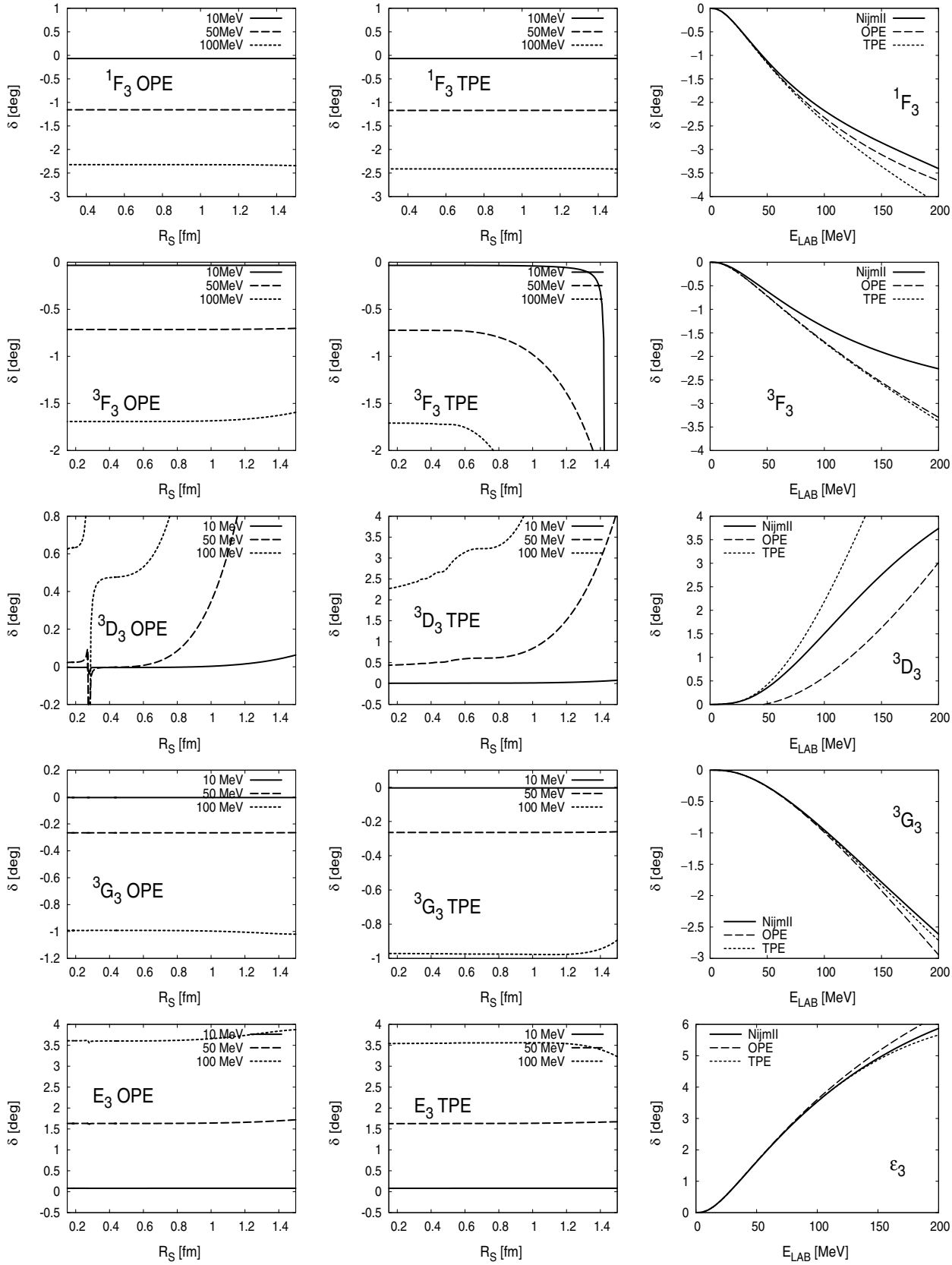

FIG. 5. Same as Fig. 2, but for $j = 3$.

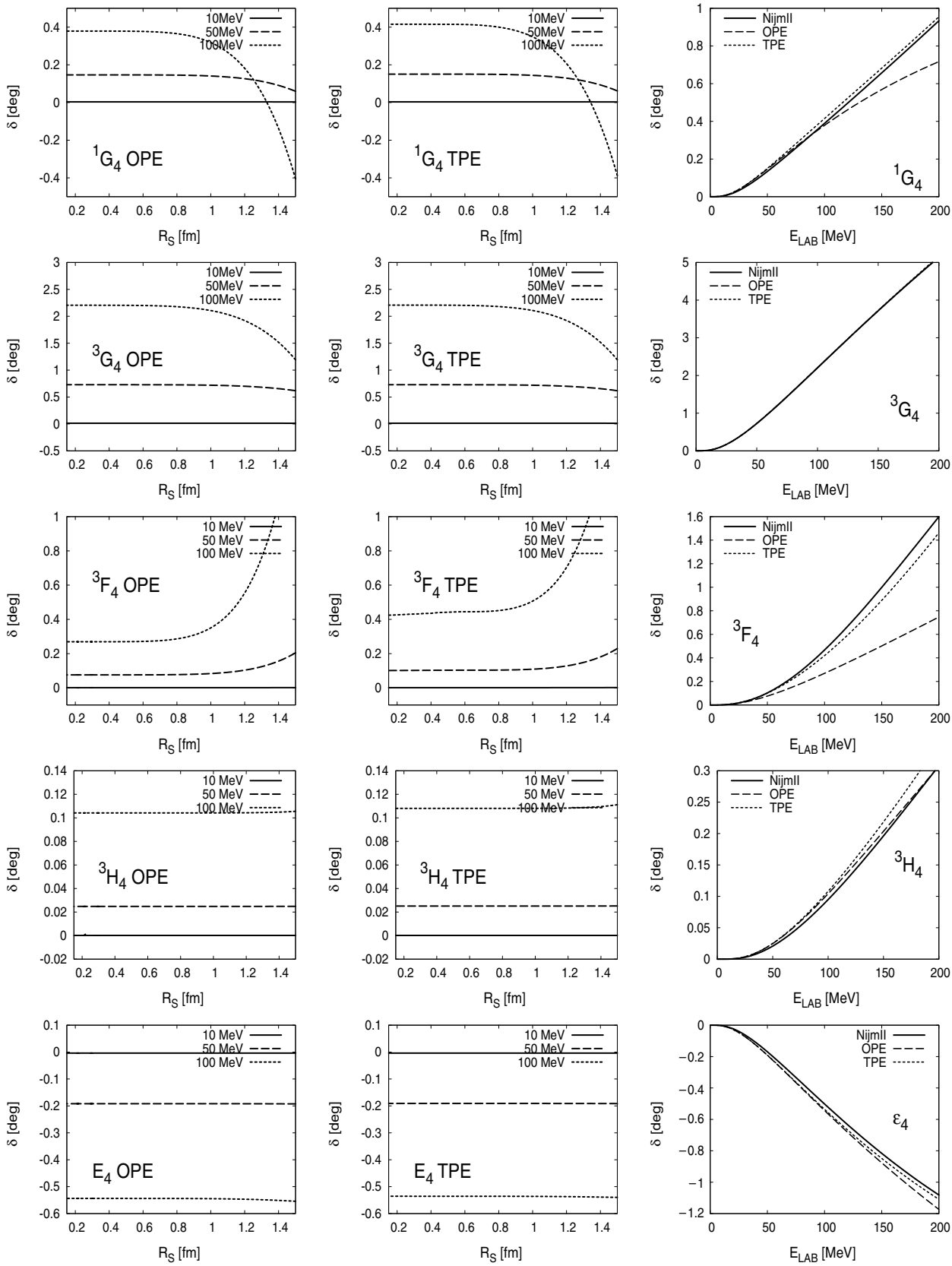

FIG. 6. Same as Fig. 2, but for $j = 4$.

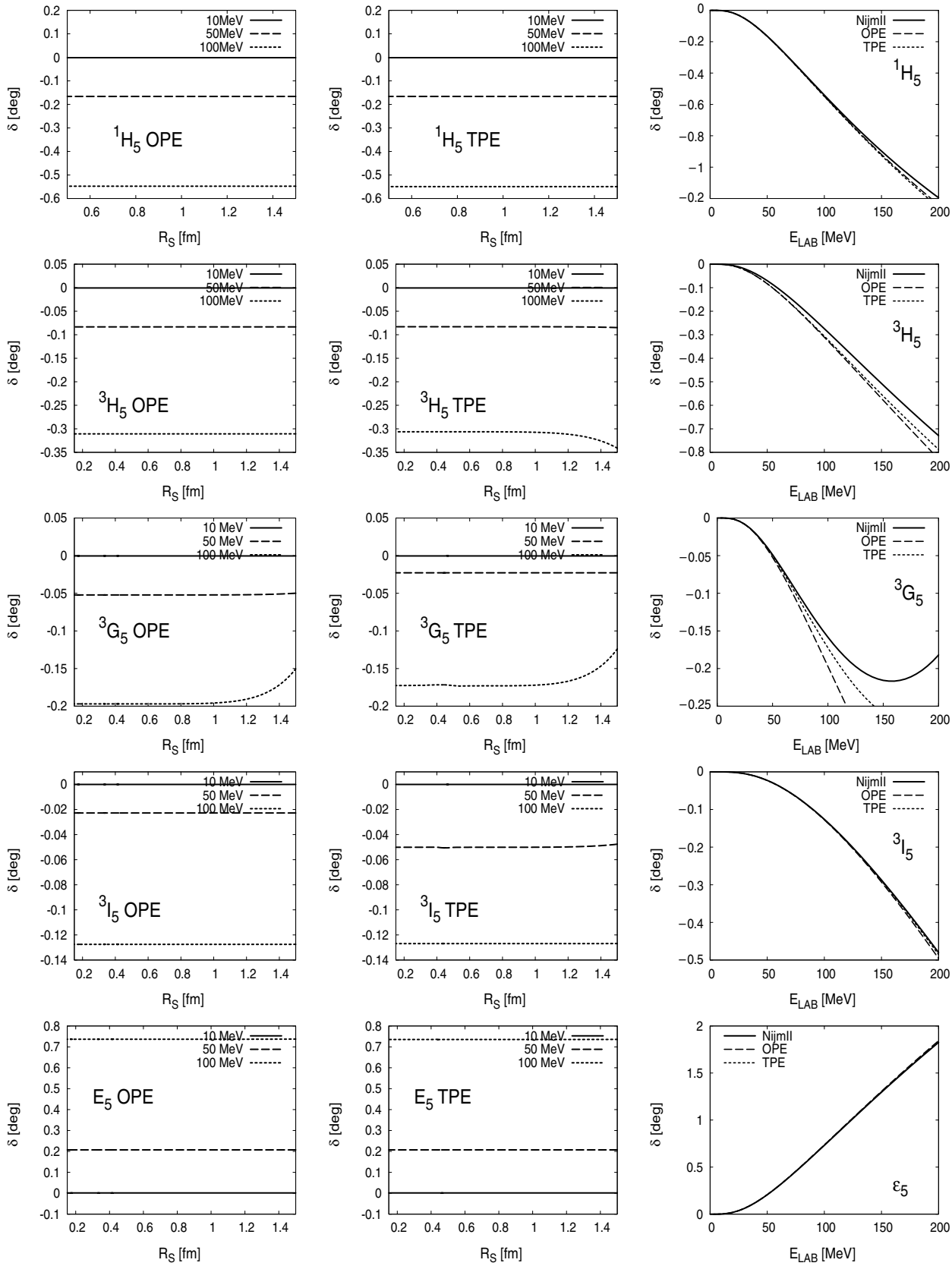

FIG. 7. Same as Fig. 2, but for $j = 5$.

($\sim r$) and irregular (~ 1) solutions at the origin.[8] A similar behavior can be found on other singlet waves in which the OPE potential also behaves as $1/r$, but is highly attenuated by the influence of the centrifugal barrier.

Finally, let us note that in some channels, the phase shifts exhibit a very strong dependence on the regulator.[9]

D. Renormalized phase shifts

1. LO (OPE)

In Figs. 2–7 we also compare the OPE (LO), the NNLO TPE, and the Nijmegen phase-shift analysis [46,47]. As noted in Table II, in some cases with attractive singular potentials, some scattering lengths must be specified in order to determine the phase shifts; but for repulsive singular potentials, the scattering lengths and hence the phase shifts are fully determined from the potential. In the coupled channel case, where only one parameter should be fixed, we have chosen, as indicated in Table II, to take the scattering length of the corresponding partial wave with the lower orbital angular momentum. As we see from Figs. 2–7, OPE does a relatively good job for the phases when compared to the NijmII results, up to a reasonable energy. This calculation extends our previous results [41] using the same regularization for the singlet $^1S_0$ and triplet $^3S_1$-$^3D_1$ channels.

The LO results corresponding to static OPE potentials have also been obtained recently in momentum space by a solution of the Lippmann-Schwinger equation in Ref. [42] for $j \leqslant 3$. These authors see that in the limit $\Lambda \to \infty$ (in practice, $\Lambda = 4$ GeV), it is always possible to adjust a counterterm in such a way that the phase shifts are cutoff independent. They also find that the needed counterterm does not correspond to the expectations based on Weinberg's dimensional power counting argument, so one is forced to promote counterterms which are of higher order in Weinberg's counting to make the theory free of short distance ambiguities. This proposal not only fits quite naturally into our analysis of short distance boundary conditions, but also can be anticipated by just looking at the short distance behavior of the potential. In general, we reproduce their results for the phase shifts using our boundary condition regularization (our shortest distance cutoff is typically $a = 0.1$ fm for OPE). This is precisely one of the points of renormalization; different regularization methods should yield identical results when the regulator is removed provided the same renormalization conditions are imposed. Note that in our case, whenever a scattering length must be provided we exactly construct the phase shift so as to reproduce the threshold behavior of the Nijmegen phases [46,47] by exactly fixing the scattering length (the renormalization condition). This requires solving the zero-energy problem by integrating in with the given scattering length and matching at short distances the finite-energy problem to finally determine the phase shift by integrating out. In this approach, we never make a fit. In the approach of Ref. [42], counterterms are adjusted to fit the phases in the region around threshold. Although this is in spirit the same renormalization condition to fix the counterterms, we expect some numerical discrepancies, because the threshold parameters in Ref. [42] may be slightly different than ours.

2. NLO (TPE)

Regarding NLO, we do not show the results because they fail completely to describe the data in the triplet $^3S_1$-$^3D_1$ channel. The problem we found already [43] in the triplet $^3S_1$-$^3D_1$ channel persists in other channels; the short distance behavior of the NLO potential corresponds to $1/r^5$ repulsive eigenpotentials. This feature explains the relatively small maximal cutoffs allowed in NLO calculations in momentum space. As stressed in our previous work, there are at least two scenarios in which the problem may be overcome. One possibility appeals to the role of the Δ resonance and the fact that its contribution to c_3 and c_4 scales as the inverse of the $N\Delta$ splitting $\Delta \sim 2m_\pi$ as found in Refs. [3,13,53]. In the Δ counting, the c_3 and c_4 contributions to the NNLO deltaless potential become actually NLO contributions, and the short distance behavior becomes a $1/r^6$ attractive singularity. The second scenario has to do with the influence of relativity beyond a truncated heavy baryon expansion, since according to Refs. [25–27] one has a relativistic $1/r^7$ van der Waals short distance behavior with attractive-repulsive eigenpotentials, meaning that as in the OPE case one has one free parameter. Calculations taking into account these effects in all partial waves are currently underway [54].

3. NNLO (chiral-TPE)

We turn now to the NNLO calculation which contains the chiral constants c_1, c_3, and c_4 (see, e.g., Table I) and for definiteness we will use mainly set IV [8] in our analysis.[10] Results for the TPE renormalized phase shifts are presented in Figs. 2–7. Some expected features do indeed occur. Peripheral waves are slightly modified by going from OPE to the chiral TPE potential. On the other hand, low partial waves are also improved in the low-energy region. For instance, the $^1S_0$ phase has an attractive singular interaction, requiring fixing the

[8] Anyway, the lack of a clear plateau in this wave becomes obvious in the coordinate space treatment. Assuming the relationship $\Lambda \sim 1/(0.48 R_S)$ for a Gaussian cutoff (see footnote 7) between the momentum and coordinate space cutoffs, a linear dependence of the phase shifts on the R_S coordinate cutoff would map into a $1/\Lambda$ dependence in momentum space, which might be regarded as a plateau in a sufficiently thin cutoff window. Note that going from $R_s = 0.2$ fm to $R_s = 0.1$ fm corresponds equivalently to double the momentum space cutoff from ~ 2 to ~ 4 GeV.

[9] The jump in the evolution of the OPE potential in the $^3D_3$ channel around $R_S = 0.3$ fm (Fig. 5) resembles a coupled channel resonance, corresponding to tunneling across the centrifugal barrier into the short distance attractive singularity.

[10] The NNLO potential contains parameters which are relating πN and NN data in some intricate way. We are using parameter set IV [8] because it nicely reproduces the deuteron properties. One could, of course, improve on this by a large-scale fit to the data.

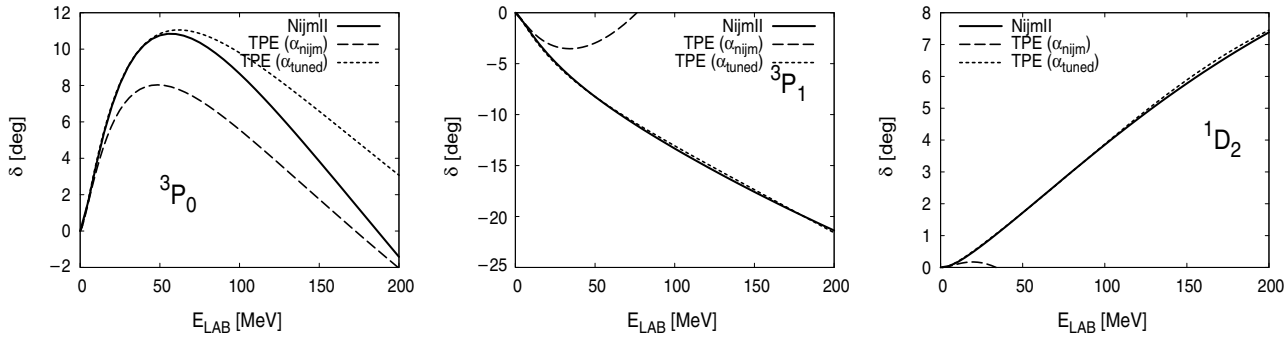

FIG. 8. Dependence of some phases for the chiral TPE potential on the scattering lengths compared to the NijmII phases [46,47]. We use set IV of chiral constants. Label TPE ($\alpha_{\rm nijm}$) means scattering lengths of Table II are taken as deduced in Ref. [48], while TPE ($\alpha_{\rm tuned}$) stands for the values tuned to fit the phases in the intermediate-energy region. For $^3P_0$, we take $\alpha_1 = -2.670\,\text{fm}^3$; for $^3P_1$, $\alpha_1 = 1.692\,\text{fm}^3$; for $^1D_2$, $\alpha_2 = -1.666\,\text{fm}^5$.

scattering length. The difference in the curves is mainly related to the difference in the effective range, which improves when going from OPE to TPE [43]. This is a rather general feature; the error at low energies is controlled by the low-energy threshold parameters such as the effective range. If one looks at the $^3P_0$ channel, we see that there is improvement but not as dramatic as in the $^1S_0$ channel.

As we have said, in singular repulsive channels, which at NNLO correspond to the $^1P_1$, $^1F_3$, and $^1H_5$ singlet states and to the $^3P_2$-$^3F_2$ and $^3F_4$-$^3H_4$ triplet states, the phase shift and the scattering length are entirely determined by the potential. So, these phases are a good place in which to study the influence of different values for the chiral constants c_1, c_3, and c_4, presented in Table I. In Fig. 8, we show this dependence for these special partial waves. As we see, the $^1P_1$ phase exhibits a strong dependence on the parameter set, while $^1F_3$ and $^1H_5$ are less sensitive to this particular choice. The strong dependence in the $^1P_1$ channel suggests that this may be an ideal place in which to fit the chiral constants, since the scattering lengths are fixed. We will not attempt such a determination of the chiral constants here because that would require realistic error estimates of the phase shifts.

If we restrict ourselves to the spin singlet channels, we see that there is very good agreement for higher peripheral waves, $^1H_5$, $^1G_4$, and $^1F_3$. This is expected from perturbative calculations. Note, however, that unlike perturbation theory, we fix by construction the scattering lengths for the cases of singular and attractive potentials. Some intermediate waves, such as $^1D_2$, for which potential is singular attractive, are badly reproduced despite the fact that the threshold behavior is in theory reproduced, since we use the corresponding scattering length as input. Actually, for these waves the TPE result seems to worsen the OPE prediction. Presumably this is an indication of either the inadequacy of the (NijmII) scattering lengths used as input for NNLO or the importance of N^{3}LO contributions. Let us note that the NijmII potential does not incorporate explicit TPE effects in their long range part. In fact, if we take a slightly different scattering length, $\alpha_2 = -1.666\,\text{fm}^5$, instead of the values deduced in Ref. [48] ($\alpha_2 = -1.389\,\text{fm}^5$) for the NijmII potential, a rather good agreement with the Nijmegen analysis is obtained for the $^1D_2$ phase shift (see similar results for $^3P_0$ and $^3P_1$ waves in Fig. 9). Although the small difference between the fitted and experimental values for the scattering length could also be explained by N^{3}LO corrections, suggesting that they are not large, a definite conclusion cannot be drawn in the absence of a large-scale fit.[11]

[11]This also applies to the nonstatic OPE corrections which account for about 0.1° at $E_{\rm LAB} = 200$ MeV. The effect can be mocked up by even tinier readjustments of both the scattering lengths and the chiral couplings c_1, c_3, and c_4 than deduced from inaccuracies in the NijmII potentials.

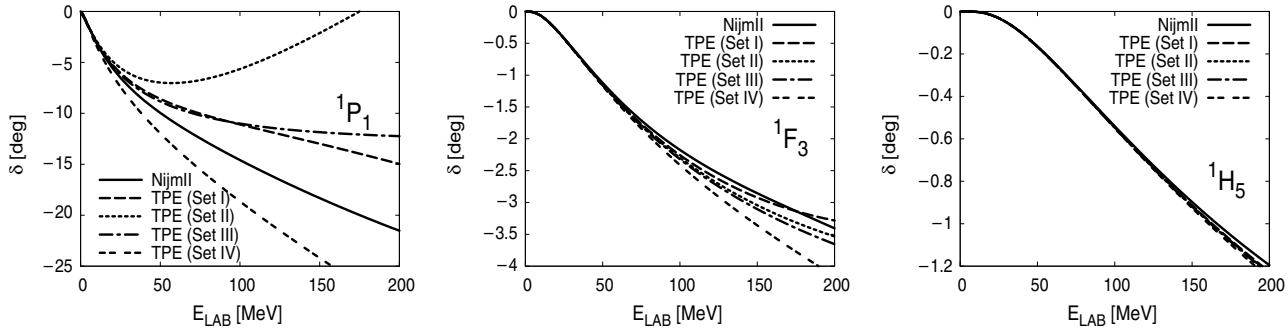

FIG. 9. Dependence of NNLO (SYM-nuclear bar) phases on chiral constants. These are the only channels for which the potential is singular repulsive.

These general trends are confirmed in the triplet channels, where in high partial waves there is an overall improvement when going from OPE to TPE. In some cases, as in the $^3D_2, \epsilon_2, ^3P_2$, and $^3F_2$, the improvement is rather satisfactory all over the energy range. However, the theory has notorious problems in the $^3P_1$ and ϵ_1 and to a lesser extent in the $^3D_3$ and E_1 channels if one insists on keeping the scattering lengths of the NijmII potential. As before, small changes in the scattering lengths allow for an overall improved description, as can be deduced from Fig. 8 in some particular cases (see also Fig 1). This suggests that higher orders in the potential may be needed. This fact was pointed out in our previous work on the central phases, where the NNLO potential almost made the effective range, although there was a statistically significant discrepancy to the experimental number, which called for the inclusion of N^{3}LO terms. This may possibly happen also in some higher partial waves, and it would be interesting to see whether improved long distance potentials might account for the observed discrepancies to phase shifts provided the scattering lengths are kept to their physical values.

As we have shown (see Fig. 8), small changes in the scattering lengths indeed allow a better description of the phases in the intermediate-energy region. On the other hand, we would expect our description to become increasingly better for lower energies. This situation is a bit disconcerting. Given the similarity between the scattering lengths computed in Ref. [48] for the NijmII and Reid93 potentials, it seems unlikely that potential models yield a completely off value for the α's in noncentral waves, but one must admit that errors will in general be larger than suggested by the difference between these two potential values, as already argued above. If one takes into account the fact that both potentials include similar long range physics, this means that the true error could be larger due to systematic uncertainties in their short range part (non-OPE).

Nevertheless, let us mention that current calculations involving chiral potentials not only ignore this possible disagreement at threshold but also in fact modify the corresponding scattering lengths since the counterterms are determined by a fit to the phase shifts in the region above threshold with no obvious control on the low-energy parameters (see, e.g., Ref. [42]). The arguments above do not prove that taking slightly different scattering lengths than those suggested by the high quality potentials is a legitimate operation, but at least they show that no more assumptions are made. From this viewpoint, it might be profitable to study the impact on those calculations of either imposing exact threshold behavior or, alternatively, evaluating the threshold parameters themselves.

E. Remarks on the perturbative nature of peripheral waves

The numerical coincidence of our nonperturbative calculations with perturbation theory expectations [4,24], although quite natural on physical grounds, deserves some explanation on the basis of the formalism and the relevance of short distance singularities. Indeed, the attractive character of the singular NNLO potentials at the origin implies a nontrivial boundary condition of the form of Eq. (24), which cannot be reproduced to any given order in perturbation theory, at least without the inclusion of extra counterterms in the perturbative expansion, a point which will be further discussed at the end of this section. This point was previously illustrated in Ref. [36] for s waves and also in our previous work on the renormalization of the OPE [41] by comparing the exact deuteron wave functions with the perturbative ones. There, one observes that the first-order perturbative calculation provides finite results, but the expansion at second order produces divergent results because of the short distance nonnormalizable D-wave component. Thus, observables cannot, strictly speaking, be analytical functions of the coupling (for the purpose of discussion we could visualize the problem by thinking of singularities of the sort $g^2 + g^4 \log g^2$). This does not mean that for the physical range of couplings the nonanalytical contribution is necessarily large numerically. For instance, in the deuteron channel, the residual nonanalytical higher order terms happens to be numerically sizable even for a weakly bound deuteron.

Based on the results of Ref. [41], there is no reason to expect that higher partial waves will not exhibit this failure of perturbation theory at some finite order. Nevertheless, the perturbative short distance behavior of higher partial waves tames the singularity because of the kinematic r^l suppression. This is a perturbative long distance feature in which the centrifugal barrier dominates. The point is that this short distance behavior is not invariant order by order in strict perturbation theory for a singular potential, and, actually, one finds a short distance enhancement of the wave function even in perturbation theory. So, one expects that the perturbation theory on a singular potential will diverge at some finite order also for high partial waves. In Appendix C, we show that this is indeed the case; for a singular potential diverging like $1/r^n (n > 2)$ and a partial wave with angular momentum l, the perturbative expansion diverges at kth order in perturbation theory, provided $k > (2l + 1)/(n - 2)$. This estimate provides the order at which, if desired, a long distance perturbation theory on boundary conditions might be applied as discussed previously for the deuteron channel [41]. Using the techniques developed in Ref. [43] to make perturbation theory on distorted OPE central waves, it would be interesting to see, as claimed by the renormalization arguments put forward by Birse on the OPE [55], whether such an expansion is indeed possible.

Having established that perturbation theory will diverge at some finite order, we would now like to understand why it still can accurately represent the full nonperturbative solutions obtained numerically. The reason can be found in the very efficient way in which the short distance singularity of the potential makes short distances inessential in the wave function for the regular nonperturbative solution. For high angular momenta and attractive singular potentials, the wave function senses the singularity after tunneling through the barrier, an exponentially suppressed effect. In perturbation theory, the effect is just substituted by the core provided by the centrifugal barrier.

IV. CONCLUSIONS

In the present paper, we have analyzed the renormalization of noncentral waves for NN scattering for the OPE and

chiral TPE potentials. This calculation extends our previous studies on central phases and the deuteron for OPE and TPE potentials presented in Refs. [41,43], respectively. As already stressed in those works, the requirement of finiteness of the scattering amplitude as well as the orthogonality of wave functions impose tight constraints on the allowed structure of counterterms for a given potential. Using the standard Weinberg counting for the potential, the counterterm structure is deduced and does not generally coincide with the naive expectations. In some cases, counterterms which are higher order in the Weinberg counting must be allowed [41,42], whereas in some other cases allowed counterterms must be excluded [43]. Finite cutoff calculations based on the Weinberg counting allow one to introduce counterterms which are usually readjusted to globally fit the data but are forbidden by finiteness and orthogonality, in renormalized calculations. The success of the original counting relies heavily on keeping the cutoff finite, while at the same time, it is usually emphasized that low-energy physics does not depend crucially on short distance details. As we have argued, these two facts are mutually contradicting; the standard Weinberg counting is incompatible with exact renormalization, i.e., removing the cutoff, as was suggested in Ref. [56] within a perturbative setup and shown in Ref. [42] nonperturbatively, at least in the heavy baryon expansion and when only nucleons and pions are taken into account. This feature changes when relativistic effects and Δ degrees of freedom are taken into account, showing that perhaps renormalization, i.e., the independence on short distance details, may be a strong condition on admissible potentials. In this regard, we find that, as one would expect, the cutoff dependence is milder for the chiral TPE potential than for the OPE potential. This suggests that higher order corrections become even more cutoff independent. Indeed, the finite cutoff N^{3}LO calculations of Ref. [11] do exhibit this feature in spite of the strong cutoff dependence observed at lower orders.

Using this modified Weinberg counting, the quality of the agreement and improvement depends on the particular partial wave. High partial peripheral waves, when treated nonperturbatively reproduce the data fairly well, and deviations from OPE to TPE are small, as one would expect in a perturbative treatment. Nevertheless, we have also shown that regardless of the orbital angular momentum, there is always a limit to the order in perturbation theory for which finite results are obtained. The divergence is related to an indiscriminate use of the perturbative expansion and not to an intrinsic deficiency in the definition of the scattering amplitude. Thus, also for peripheral waves, the phase shifts are perturbatively renormalizable with an increasing number of counterterms, whereas they are nonperturbatively renormalizable with a finite number of counterterms. This result extends a similar observation for the deuteron [40,41]. Nevertheless, we have also argued as to why convergent perturbative calculations to finite order are useful and may even provide accurate descriptions when compared with nonperturbative results.

Unlike naive expectations, it is not always true that after renormalization the NNLO TPE phases improve over OPE ones if one insists on keeping the scattering lengths required by finiteness to the same physical values as those extracted [48] from the high quality Nijmegen potentials [47]. This renormalization condition at zero energy was adopted to highlight the difference between these potentials [47] and the chiral NNLO singular potentials [4]. Remarkably, using zero energy to fix the parameters has never been considered before within the chiral potentials approach to NN scattering; thus, some of the problems we find and discuss have not even been identified so far. Actually, we find that some partial waves such as $^1D_2$ and $^3P_1$ are particularly sensitive to the value of the scattering length. In fact, it is found that small deviations of the scattering lengths at the few percent level in these partial waves improve dramatically the description in the intermediate-energy region. The improvement can also be achieved in other partial waves by suitably tuning the scattering lengths in all the channels characterized by singular attractive interactions. This means that the absolute error is small up to $E_{\rm LAB} \sim 100$ MeV. Three-pion exchange effects should become relevant at about c.m. momentum of $k = 3m/2$, which corresponds approximately to this laboratory energy. The modification corresponds to changing the renormalization condition to some finite energy or to maximizing the overlap between the chiral phase shifts and the fitted ones in a given energy window, very much along the lines pursued in previous works. However, changing the scattering lengths produces large relative errors near the threshold. At this point, the discussion on errors in the phase shifts becomes a crucial matter, particularly in the low-energy region. In this regard, it seems likely that the difference in low-energy threshold parameters determined in Ref. [48] for the Reid93 and NijmII in all partial waves with $j \leqslant 5$ provides a lower bound for the true error. Obviously, a meticulous error analysis of these threshold parameters would be very helpful.

We have also found that some partial waves, with repulsive singular interactions and where no free scattering lengths are allowed, are particularly sensitive to the choice of chiral constants c_1, c_3, and c_4. This suggests that a fit of the chiral constants to these partial waves may be possible. To do so, a realistic estimate of the errors of the phase shifts would again be mandatory. According to our findings on the deuteron for the chiral TPE potential [43], it is quite likely that, if such an error estimate were reliably done, theoretical determinations for deuteron observables with unprecedented precision based on chiral potentials might be achieved. This issue is currently under consideration and is left for future research [57].

From a practical viewpoint, there is a potential disadvantage in requiring exact renormalization for the approximated long distance chiral potentials, because of the tight constraints imposed by finiteness on the short distance behavior of the wave functions. To some extent, although the chiral potentials are motivated by the effective field theory idea, these additional conditions remind us also of aspects of renormalization of fundamental theories. This is not entirely surprising since we expect the chirally based potentials to resemble the correct long range NN physics, at least at sufficiently long distances. For instance, OPE is the leading long distance contribution, while full TPE would be a subleading part, which is known in an approximate manner within the current ChPT schemes based on dimensional power counting. Nevertheless, the essential difference is that nonperturbative dimensional transmutation,

i.e., the generation of dimension-full parameters not encoded in the potential, occurs because of the singular and attractive nature of long distance interactions already at the lowest order approximation consisting of OPE. This nonperturbative renormalizability is the essential feature that makes this problem particularly tough and so distinct from the previous experience of perturbative renormalization on effective field theories or finite cutoff representations of the problem.

The present work shows not only that the theoretical requirement of renormalizability can be implemented as a matter of principle and as a practical way of controlling short distance ambiguities in the predictions of chiral perturbation theory for the study of NN scattering, but also that interesting physical and phenomenological insights are gathered from such an investigation. We have shown the conditions under which such a program can successfully be carried out as a possible alternative and model-independent way of describing the data by using very indirect, but essential, information on the implications of chiral symmetry for the NN problem below the pion production threshold.

ACKNOWLEDGMENTS

We have profited from lively and stimulating discussions with the participants at "Nuclear Forces and QCD: Never the Twain Shall Meet ? " at ECT* in Trento. We would like to thank Andreas Nogga for pointing out an error in the $^1S_0$ phase-shift plot. This work is supported in part by the Spanish DGI and FEDER funds with Grant No. FIS2005-00810, Junta de Andalucía Grant No. FQM-225, and EU RTN Contract CT2002-0311 (EURIDICE).

APPENDIX A: POTENTIALS

For completeness, we list here the potentials found in Ref. [4] and used in this paper. In coordinate space, the general form of the potential is written as

$$\begin{aligned}\mathcal{V}_{NN} &= V_C(r) + \vec{\tau}_1\cdot\vec{\tau}_2 W_C(r) \\ &+ [V_S(r) + \vec{\tau}_1\cdot\vec{\tau}_2 W_S(r)]\,\vec{\sigma}_1\cdot\vec{\sigma}_2 \\ &+ [V_T(r) + \vec{\tau}_1\cdot\vec{\tau}_2 W_T(r)]\,(3\vec{\sigma}_1\cdot\hat{r}\vec{\sigma}_2\cdot\hat{r} - \vec{\sigma}_1\cdot\vec{\sigma}_2) \\ &+ [V_{LS}(r) + \vec{\tau}_1\cdot\vec{\tau}_2 W_{LS}(r)]\,\vec{L}\cdot\vec{S}. \end{aligned} \tag{A1}$$

For states with good total angular momentum, one obtains

$$U^{0j}_{jj}(r) = M\,[(V_C - 3V_S) + \tau(W_C - 3W_S)]\,, \tag{A2}$$

$$\begin{aligned}U^{1j}_{jj}(r) &= M[(V_C + V_S - V_{LS}) + \tau(W_C + W_S - W_{LS}) \\ &+ 2(V_T + \tau W_T)], \end{aligned} \tag{A3}$$

$$\begin{aligned}U^{1j}_{j-1,j-1} &= M[(V_C + \tau W_C + V_S + \tau W_S) + (j-1) \\ &\times (V_{LS} + \tau W_{LS}) + \frac{2(j-1)}{2j+1}(V_T + \tau W_T)], \end{aligned} \tag{A4}$$

$$U^{1j}_{j-1,j+1} = -\frac{6\sqrt{j(j+1)}}{2j+1} M\,(V_T + \tau W_T)\,, \tag{A5}$$

$$\begin{aligned}U^{1j}_{j+1,j+1} &= M[(V_C + \tau W_C + V_S + \tau W_S) + 2(j+2) \\ &\times (V_{LS} + \tau W_{LS}) + \frac{2(j+2)}{2j+1}(V_T + \tau W_T)], \end{aligned} \tag{A6}$$

with $\tau = 2T(T+1) - 3$. Remember that Fermi-Dirac statistics requires $(-1)^{L+S+T} = -1$.

The LO (OPE) potentials read ($x = m_\pi r$)

$$W_S^{\rm OPE} = \frac{g^2 m^3}{48\pi f^2}\frac{e^{-x}}{x}, \tag{A7}$$

$$W_T^{\rm OPE} = \frac{g^2 m^3}{48\pi f^2}\frac{e^{-x}}{x}\left(3 + \frac{3}{x} + \frac{1}{x^2}\right), \tag{A8}$$

all others being zero.

The nonvanishing NNLO (TPE) potentials are given by

$$\begin{aligned}V_C^{\rm TPE}(r) &= \frac{3g^2m^6}{32\pi^2 f^4}\frac{e^{-2x}}{x^6}\left\{\left(2c_1 + \frac{3g^2}{16M}\right)x^2(1+x)^2 + \frac{g^5x^5}{32M}\right. \\ &\left. + \left(c_3 + \frac{3g^2}{16M}\right)(6 + 12x + 10x^2 + 4x^3 + x^4)\right\}, \\ W_T^{\rm TPE}(r) &= \frac{g^2m^6}{48\pi^2 f^4}\frac{e^{-2x}}{x^6}\left\{-\left(c_4 + \frac{1}{4M}\right)(1+x)(3+3x\right. \\ &\left. + x^2) + \frac{g^2}{32M}\left(36 + 72x + 52x^2 + 17x^3 + 2x^4\right)\right\}, \\ V_T^{\rm TPE}(r) &= \frac{g^4m^5}{128\pi^3 f^4 x^4}\left\{-12K_0(2x) - (15 + 4x^2)K_1(2x)\right. \\ &\left. + \frac{3\pi m e^{-2x}}{8Mx}(12x^{-1} + 24 + 20x + 9x^2 + 2x^3)\right\}, \\ W_C^{\rm TPE}(r) &= \frac{g^4m^5}{128\pi^3 f^4 x^4}\left\{[1 + 2g^2(5 + 2x^2) - g^4(23 + 12x^2)]\right. \\ &\times K_1(2x) + x[1 + 10g^2 - g^4(23 + 4x^2)]K_0(2x)\,, \\ &+ \frac{g^2 m\pi e^{-2x}}{4Mx}[2(3g^2 - 2)(6x^{-1} + 12 + 10x \\ &\left. + 4x^2 + x^3)] + g^2x(2 + 4x + 2x^2 + 3x^2)\right\}, \\ V_S^{\rm TPE}(r) &= \frac{g^4m^5}{32\pi^3 f^4}\left\{3xK_0(2x) + (3 + 2x^2)K_1(2x)\right. \\ &\left. - \frac{3\pi m e^{-2x}}{16Mx}(6x^{-1} + 12 + 11x + 6x^2 + 2x^3)\right\}, \\ W_S^{\rm TPE}(r) &= \frac{g^2m^6}{48\pi^2 f^4}\frac{e^{-2x}}{x^6}\left\{\left(c_4 + \frac{1}{4M}\right)(1+x)(3+3x+2x^2)\right. \\ &\left. - \frac{g^2}{16M}(18 + 36x + 31x^2 + 14x^3 + 2x^4)\right\}, \\ V_{LS}^{\rm TPE}(r) &= -\frac{3g^4m^6}{64\pi^2 Mf^4}\frac{e^{-2x}}{x^6}(1+x)(2+2x+x^2), \\ W_{LS}^{\rm TPE}(r) &= \frac{g^2(g^2-1)m^6}{32\pi^2 Mf^4}\frac{e^{-2x}}{x^6}(1+x)^2, \end{aligned} \tag{A9}$$

where K_0 and K_1 are modified Bessel functions. The NLO terms are obtained by dropping all terms in $1/M$ and c_1, c_3, and c_4.

APPENDIX B: LEADING SINGULARITIES IN THE SHORT DISTANCE EXPANSION

The determination of the short distance behavior from the full potentials is straightforward, but it is necessary to determine the number of independent parameters in every channel and at any level of approximation. For a quick reference we list the leading singularity behavior in Table IV.

APPENDIX C: THE DIVERGENCE OF PERTURBATION THEORY FOR PERIPHERAL WAVES

In this appendix, we show that for a singular, attractive or repulsive, potential at the origin which diverges like $1/r^n$, there is always a finite order in perturbation theory where the phase shift diverges, regardless of the particular value of the angular momentum. Let us consider for simplicity the single channel case. The radial equation can be transformed into the integral equation

$$u_l(r) = \hat{j}_l(kr) + \int_0^\infty G_{k,l}(r,r')U(r')u_l(r')dr', \qquad \text{(C1)}$$

where $G_{k,l}$ is the Green function given by

$$kG_{k,l}(r,r') = \hat{j}_l(kr)\hat{y}_l(kr')\theta(r'-r) + \hat{j}_l(kr')\hat{y}_l(kr)\theta(r-r'), \qquad \text{(C2)}$$

where $\theta(x)$ is the Heavyside step function, $\theta(x) = 1$ for $x \geqslant 0$ and $\theta(x) = 0$ for $x < 0$, and $\hat{j}_l(x) = x j_l(x)$ and $\hat{y}_l(x) = x y_l(x)$ are the regular and singular reduced spherical Bessel functions, respectively. To regularize the lower limit of integration in Eq. (C1), one may assume a short distance regulator which will eventually be removed. The phase shift is given by

$$\tan\delta_l = -\frac{1}{k}\int_0^\infty \hat{j}_l(kr)U(r)u_l(r). \qquad \text{(C3)}$$

In perturbation theory, the successive iteration of Eq. (C1) produces the Born series

$$\tan\delta_l = -\frac{1}{k}\int_0^\infty dr\left[\hat{j}_l(kr)\right]^2 U(r) - \frac{1}{k}\int_0^\infty drdr'\hat{j}_l(kr)U(r)U(r')G_{k,l}(r,r')j_l(kr') + \cdots. \qquad \text{(C4)}$$

For our purposes of proving the divergence of perturbation theory, it is sufficient to analyze the low-energy limit. Using $\delta_l \to -\alpha_l k^{2l+1}$ and using known properties of the Bessel functions

$$\hat{j}_l(x) \to \frac{x^{l+1}}{(2l+1)!!}, \qquad \hat{y}_l(x) \to -\frac{(2l-1)!!}{x^l}, \qquad \text{(C5)}$$

Green's function becomes

$$-(2l+1)G_{0,l}(r,r') = \frac{r^{l+1}}{r'^l}\theta(r'-r) + \frac{r'^{l+1}}{r^l}\theta(r-r'), \qquad \text{(C6)}$$

TABLE IV. Leading short distance singularity of the NN reduced potentials, $U = 2\mu V$, Eq. (1) to LO, NLO, and NNLO for all channels considered in this work. The signs of the coefficients for the one channel case (singlet and triplet) or the eigenvalues for the triplet coupled channel case determine the number of independent parameters. $\bar{c}_3 = c_3 M$ and $\bar{c}_4 = M c_4$ are the dimensionless chiral constants.

Wave	LO	NLO	NNLO
$^1S_0$	$-\frac{g^2m^2M}{16\pi f^2}\frac{1}{r}$	$\frac{(1+10g^2-59g^4)M}{256\pi^3 f^4}\frac{1}{r^5}$	$\frac{3g^2(-4+24\bar{c}_3-8\bar{c}_4+15g^2)}{128\pi^2 f^4}\frac{1}{r^6}$
$^3P_0$	$-\frac{g^2M}{4\pi f^2}\frac{1}{r^3}$	$\frac{(1+10g^2+49g^4)M}{256\pi^3 f^4}\frac{1}{r^5}$	$\frac{g^2(12+72\bar{c}_3+40\bar{c}_4+g^2)}{128\pi^2 f^4}\frac{1}{r^6}$
$^1P_1$	$\frac{3g^2m^2M}{16\pi f^2}\frac{1}{r}$	$\frac{3(-1-10g^2+11g^4)M}{256\pi^3 f^4}\frac{1}{r^5}$	$\frac{9g^2(4+8\bar{c}_3+8\bar{c}_4-3g^2)}{128\pi^2 f^4}\frac{1}{r^6}$
$^3P_1$	$\frac{g^2M}{8\pi f^2}\frac{1}{r^3}$	$\frac{(1+10g^2-41g^4)M}{256\pi^3 f^4}\frac{1}{r^5}$	$\frac{g^2(-2+36\bar{c}_3-4\bar{c}_4+19g^2)}{64\pi^2 f^4}\frac{1}{r^6}$
$^3S_1$	0	$\frac{3(-1-10g^2+27g^4)M}{256\pi^3 f^4}\frac{1}{r^5}$	$-\frac{3g^2(-4-24\bar{c}_3+8\bar{c}_4+3g^2)}{128\pi^2 f^4}\frac{1}{r^6}$
$^3D_1$	$\frac{3g^2}{8f^2\pi}\frac{1}{r^3}$	$\frac{3(-1-10g^2+37g^4)M}{256\pi^3 f^4}\frac{1}{r^5}$	$\frac{9g^2(-1+2\bar{c}_3-2\bar{c}_4+2g^2)}{32\pi^2 f^4}\frac{1}{r^6}$
E_1	$-\frac{3g^2}{4\sqrt{2}f^2\pi}\frac{1}{r^3}$	$-\frac{15g^4M}{64\sqrt{2}f^4\pi^3}\frac{1}{r^5}$	$\frac{-3g^2(-4-16\bar{c}_4+3g^2)}{64\sqrt{2}\pi^2 f^4}\frac{1}{r^6}$
$^1D_2$	$-\frac{g^2m^2M}{16\pi f^2}\frac{1}{r}$	$\frac{(1+10g^2-59g^4)M}{256\pi^3 f^4}\frac{1}{r^5}$	$\frac{3g^2(-4+24\bar{c}_3-8\bar{c}_4+15g^2)}{128\pi^2 f^4}\frac{1}{r^6}$
$^3D_2$	$-\frac{3g^2M}{8\pi f^2}\frac{1}{r^3}$	$\frac{(1+10g^2-89g^4)M}{256\pi^3 f^4}\frac{1}{r^5}$	$\frac{g^2(-4+18\bar{c}_3-10\bar{c}_4+15g^2)}{32\pi^2 f^4}\frac{1}{r^6}$
$^3P_2$	$-\frac{g^2M}{40f^2\pi}\frac{1}{r^3}$	$\frac{(1+10g^2-5g^4)M}{256\pi^3 f^4}\frac{1}{r^5}$	$\frac{g^2(-9+90\bar{c}_3+14\bar{c}_4+5g^2)}{160\pi^2 f^4}\frac{1}{r^6}$
$^3F_2$	$-\frac{g^2M}{10\pi f^2}\frac{1}{r^3}$	$\frac{(1+10g^2+13g^4)M}{256\pi^3 f^4}\frac{1}{r^5}$	$\frac{g^2(76+360\bar{c}_3+104\bar{c}_4+175g^2)}{640\pi^2 f^4}\frac{1}{r^6}$
E_2	$\frac{3\sqrt{3}}{20\sqrt{2}\pi f^2}\frac{1}{r^3}$	$-\frac{9\sqrt{3}g^4M}{64\sqrt{2}f^4\pi^3}\frac{1}{r^5}$	$\frac{3\sqrt{3}g^2(-4-16\bar{c}_4+15g^2)}{320\sqrt{2}\pi^2 f^4}\frac{1}{r^6}$
$^1F_3$	$\frac{3g^2m^2M}{16\pi f^2}\frac{1}{r}$	$\frac{3(-1-10g^2+11g^4)M}{256\pi^3 f^4}\frac{1}{r^5}$	$-\frac{9g^2(-4-8\bar{c}_3-8\bar{c}_4+3g^2)}{128\pi^2 f^4}\frac{1}{r^6}$
$^3F_3$	$\frac{g^2M}{8\pi f^2}\frac{1}{r^3}$	$\frac{(1+10g^2-41g^4)M}{256\pi^3 f^4}\frac{1}{r^5}$	$\frac{g^2(-2+36\bar{c}_3-4\bar{c}_4+19g^2)}{64\pi^2 f^4}\frac{1}{r^6}$
$^3D_3$	$-\frac{g^2M}{28\pi f^2}\frac{1}{r^3}$	$\frac{(7+70g^2-17g^4)M}{1792\pi^3 f^4}\frac{1}{r^5}$	$-\frac{g^2(76-504\bar{c}_3-88\bar{c}_4+37g^2}{896\pi^2 f^4}\frac{1}{r^6}$
$^3G_3$	$-\frac{5g^2M}{56\pi f^2}\frac{1}{r^3}$	$\frac{(7+70g^2+73g^4)M}{1792\pi^3 f^4}\frac{1}{r^5}$	$\frac{g^2(66+252\bar{c}_3+68\bar{c}_4+155g^2)}{448\pi^2 f^4}\frac{1}{r^6}$
E_3	$\frac{3\sqrt{3}g^2M}{28\pi f^2}\frac{1}{r^3}$	$-\frac{45\sqrt{3}g^4M}{448\pi^3 f^4}\frac{1}{r^5}$	$\frac{3\sqrt{3}g^2(-4-16\bar{c}_4+15g^2)}{448\pi^2 f^4}\frac{1}{r^6}$
$^1G_4$	$-\frac{g^2m^2M}{16\pi f^2}\frac{1}{r}$	$\frac{(1+10g^2-59g^4)M}{256\pi^3 f^4}\frac{1}{r^5}$	$\frac{3g^2(-4+24\bar{c}_3-8\bar{c}_4+15g^2)}{128\pi^2 f^4}\frac{1}{r^6}$
$^3G_4$	$-\frac{3g^2M}{8\pi f^2}\frac{1}{r^3}$	$\frac{3(-1-10g^2+17g^4)M}{256\pi^3 f^4}\frac{1}{r^5}$	$\frac{3g^2(2+12\bar{c}_3+4\bar{c}_4+g^2)}{64\pi^2 f^4}\frac{1}{r^6}$
$^3F_4$	$\frac{3g^2M}{28\pi f^2}\frac{1}{r^3}$	$\frac{3(-7-70g^2+209g^4)M}{1792\pi^3 f^4}\frac{1}{r^5}$	$\frac{3g^2(76+168\bar{c}_3-88\bar{c}_4-127g^2)}{896\pi^2 f^4}\frac{1}{r^6}$
$^3H_4$	$\frac{15g^2M}{56\pi f^2}\frac{1}{r^3}$	$\frac{3(-7-70g^2+239g^4)M}{1792\pi^3 f^4}\frac{1}{r^5}$	$\frac{3g^2(-66+84\bar{c}_3-68\bar{c}_4+137g^2)}{448\pi^2 f^4}\frac{1}{r^6}$
E_4	$-\frac{9\sqrt{3}g^2M}{28\pi f^2}\frac{1}{r^3}$	$-\frac{45\sqrt{3}g^4M}{448\pi^3 f^4}\frac{1}{r^5}$	$-\frac{9\sqrt{3}g^2(-4-16\bar{c}_4+3g^2)}{448\pi^2 f^4}\frac{1}{r^6}$
$^1H_5$	$\frac{3g^2m^2M}{16\pi f2}\frac{1}{r}$	$\frac{3(-1-10g^2+11g^4)M}{256\pi^3 f^4}\frac{1}{r^5}$	$\frac{9g^2(4+8\bar{c}_3+8\bar{c}_4-3g^2)}{128\pi^2 f^4}\frac{1}{r^6}$
$^3H_5$	$\frac{g^2M}{8\pi f^2}\frac{1}{r^3}$	$\frac{1+10g^2-41g^4)M}{256\pi^3 f^4}\frac{1}{r^5}$	$\frac{g^2(-2+36\bar{c}_3-4\bar{c}_4+19g^2)}{64\pi^2 f^4}\frac{1}{r^6}$
$^3G_5$	$\frac{3g^2M}{22\pi f^2}\frac{1}{r^3}$	$\frac{3(-11-110g^2+337g^4)M}{2816\pi^3 f^4}\frac{1}{r^5}$	$\frac{3g^2(204+264\bar{c}_3-152\bar{c}_4-373g^2)}{1408\pi^2 f^4}\frac{1}{r^6}$
$^3I_5$	$\frac{21g^2M}{88\pi f^2}\frac{1}{r}$	$\frac{3(-11-110g^2+367g^4)M}{2816\pi^3 f^4}\frac{1}{r^5}$	$\frac{3g^2(-73+66\bar{c}_3-50\bar{c}_4+151g^2)}{352\pi^2 f^4}\frac{1}{r^6}$
E_5	$-\frac{9\sqrt{15}g^2M}{44\sqrt{2}\pi f^2}\frac{1}{r}$	$-\frac{45\sqrt{15}g^4M}{704\sqrt{2}\pi^3 f^4}\frac{1}{r^5}$	$-\frac{9\sqrt{15}g^2(-4-16\bar{c}_4+3g^2)}{704\pi^2 f^4}\frac{1}{r^5}$

and we get

$$(2l+1)!!^2\alpha_l = \int_0^\infty drr^{2l+2}U(r) + \frac{2}{2l+1}\int_0^\infty drr \times \int_0^r dr'(r')^{2l+2}U(r)U(r') + \cdots. \qquad \text{(C7)}$$

Since we only want to analyze the short distance behavior, we can estimate the convergence of integrals by using the finite range and singular potential $U(r) = (R/r)^n/R^2\theta(a-r)$. Thus, we see that in the first Born approximation, the integral converges for $2l+1 > n-2$, whereas the second Born approximation requires $2l+1 > 2(n-2)$. This is obviously a more stringent condition. In general, at kth order, convergence at the origin is determined by the integral

$$\int_0^\infty dr_1 r_1 U(r_1) \int_0^{r_1} dr_2 r_2 U(r_2) \cdots \int_0^{r_{k-1}} dr_k r_k^{2l+2} U(r_k), \tag{C8}$$

which is finite only for $2l+1 > k(n-2)$, a condition violated for sufficiently high k when $n > 2$. So, for $n > 2$, there will always occur a divergent contribution at a given finite order, even if the Born approximation was finite because of a high value of the angular momentum l.

[1] S. Weinberg, Phys. Lett. **B251**, 288 (1990).
[2] S. Weinberg, Nucl. Phys. **B363**, 3 (1991).
[3] C. Ordonez, L. Ray, and U. van Kolck, Phys. Rev. C **53**, 2086 (1996).
[4] N. Kaiser, R. Brockmann, and W. Weise, Nucl. Phys. **A625**, 758 (1997).
[5] M. C. M. Rentmeester, R. G. E. Timmermans, J. L. Friar, and J. J. de Swart, Phys. Rev. Lett. **82**, 4992 (1999).
[6] E. Epelbaum, W. Gloeckle, and U. G. Meissner, Eur. Phys. J. A **19**, 125 (2004).
[7] E. Epelbaum, W. Gloeckle, and U. G. Meissner, Eur. Phys. J. A **19**, 401 (2004).
[8] D. R. Entem and R. Machleidt, Phys. Rev. C **68**, 041001(R) (2003).
[9] E. Epelbaum, W. Gloeckle, and U. G. Meissner, Nucl. Phys. **A671**, 295 (2000).
[10] M. C. M. Rentmeester, R. G. E. Timmermans, and J. J. de Swart, Phys. Rev. C **67**, 044001 (2003).
[11] E. Epelbaum, W. Glockle, and U. G. Meissner, Nucl. Phys. **A747**, 362 (2005).
[12] T. A. Rijken and V. G. J. Stoks, Phys. Rev. C **54**, 2851 (1996).
[13] N. Kaiser, S. Gerstendorfer, and W. Weise, Nucl. Phys. **A637**, 395 (1998).
[14] E. Epelbaum, W. Gloeckle, and U. G. Meissner, Nucl. Phys. **A637**, 107 (1998).
[15] J. L. Friar, Phys. Rev. C **60**, 034002 (1999).
[16] K. G. Richardson, Ph.D. thesis, University of Manchester, 1999.
[17] N. Kaiser, Phys. Rev. C **61**, 014003 (2000).
[18] N. Kaiser, Phys. Rev. C **62**, 024001 (2000).
[19] N. Kaiser, Phys. Rev. C **65**, 017001 (2002).
[20] N. Kaiser, Phys. Rev. C **64**, 057001 (2001).
[21] N. Kaiser, Phys. Rev. C **63**, 044010 (2001).
[22] D. R. Entem and R. Machleidt, arXiv:nucl-th/0303017.
[23] D. R. Entem and R. Machleidt, Phys. Lett. **B524**, 93 (2002).
[24] D. R. Entem and R. Machleidt, Phys. Rev. C **66**, 014002 (2002).
[25] R. Higa and M. R. Robilotta, Phys. Rev. C **68**, 024004 (2003).
[26] R. Higa, M. R. Robilotta, and C. A. da Rocha, Phys. Rev. C **69**, 034009 (2004).
[27] R. Higa, arXiv:nucl-th/0411046.
[28] M. C. Birse and J. A. McGovern, Phys. Rev. C **70**, 054002 (2004).
[29] P. F. Bedaque and U. van Kolck, Annu. Rev. Nucl. Part. Sci. **52**, 339 (2002).
[30] N. Fettes, U. G. Meissner, and S. Steininger, Nucl. Phys. **A640**, 199 (1998).
[31] P. Buettiker and U. G. Meissner, Nucl. Phys. **A668**, 97 (2000).
[32] A. Gomez Nicola, J. Nieves, J. R. Pelaez, and E. Ruiz Arriola, Phys. Lett. **B486**, 77 (2000).
[33] A. Gomez Nicola, J. Nieves, J. R. Pelaez, and E. Ruiz Arriola, Phys. Rev. D **69**, 076007 (2004).
[34] K. M Case, Phys. Rev. **80**, 797 (1950).
[35] W. M. Frank, D. J. Land, and R. M. Spector, Rev. Mod. Phys. **43**, 36 (1971).
[36] S. R. Beane, P. F. Bedaque, L. Childress, A. Kryjevski, J. McGuire, and U. van Kolck, Phys. Rev. A **64**, 042103 (2001).
[37] T. Frederico, V. S. Timoteo, and L. Tomio, Nucl. Phys. **A653**, 209 (1999).
[38] S. R. Beane, P. F. Bedaque, M. J. Savage, and U. van Kolck, Nucl. Phys. **A700**, 377 (2002).
[39] M. Pavon Valderrama and E. Ruiz Arriola, Phys. Lett. **B580**, 149 (2004).
[40] M. P. Valderrama and E. R. Arriola, Phys. Rev. C **70**, 044006 (2004).
[41] M. P. Valderrama and E. R. Arriola, Phys. Rev. C **72**, 054002 (2005).
[42] A. Nogga, R. G. E. Timmermans, and U. van Kolck, Phys. Rev. C **72**, 054006 (2005).
[43] M. P. Valderrama and E. R. Arriola, Phys. Rev. C **74**, 054001 (2006).
[44] M. P. Valderrama and E. R. Arriola, arXiv:nucl-th/0605078.
[45] M. Pavon Valderrama and E. Ruiz Arriola, in *Proceedings of Workshop on the Physics of Excited Nucleons (NSTAR 2004), Grenoble, France, 24–27 March 2004*, edited by L. Tiator and D. Drechsel (World Scientific, 2001).
[46] V. G. J. Stoks, R. A. M. Kompl, M. C. M. Rentmeester, and J. J. de Swart, Phys. Rev. C **48**, 792 (1993).
[47] V. G. J. Stoks, R. A. M. Klomp, C. P. F. Terheggen, and J. J. de Swart, Phys. Rev. C **49**, 2950 (1994). http://nn-online.org
[48] M. Pavon Valderrama and E. Ruiz Arriola, Phys. Rev. C **72**, 044007 (2005).
[49] H. P. Stapp, T. J. Ypsilantis, and N. Metropolis, Phys. Rev. **105**, 302 (1957).
[50] J. M. Blatt and L. C. Biedenharn, Phys. Rev. **86**, 399 (1952); Rev. Mod. Phys. **24**, 258 (1952).
[51] J. J. de Swart, M. C. M. Rentmeester, and R. G. E. Timmermans, PiN Newslett. **13**, 96 (1997).
[52] J. J. de Swart, C. P. F. Terheggen, and V. G. J. Stoks, Presented at Int. Symp. on the Deuteron, Dubna, Russia, July 4–7, 1995; nucl-th/9509032.
[53] U. van Kolck, Phys. Rev. C **49**, 2932 (1994).
[54] R. Higa, M. Pavon Valderrama, and E. Ruiz Arriola (in preparation).
[55] M. C. Birse, Phys. Rev. C **74**, 014003 (2006).
[56] D. B. Kaplan, M. J. Savage, and M. B. Wise, Phys. Lett. **B424**, 390 (1998).
[57] M. Pavon Valderrama and E. Ruiz Arriola (in preparation).